Abdominal Radiology (2019) 44:1269–1294
https://doi.org/10.1007/s00261-018-1829-0

REVIEW

The hepatoduodenal ligament revisited: cross-sectional imaging spectrum of non-neoplastic conditions

Francesco Alessandrino[1,4] · Aleksandar M. Ivanovic[2] · Daniel Souza[3,4] · Amin S. Chaoui[3,5] · Jelena Djokic-Kovac[2] · Koenraad J. Mortele[1]

Published online: 17 November 2018

Abstract

Introduction The hepatoduodenal ligament is frequently involved by conditions affecting the portal triad and surrounding structures, including a vast array of non-neoplastic conditions. Due its unique location between the retroperitoneum and the peritoneal space, the hepatoduodenal ligament is also targeted by inflammatory conditions involving the retroperitoneum and the liver. Finally, the presence of lymphatics and of the biliary tracts makes the hepatoduodenal ligament a route of spread for a variety of infections. The purpose of this pictorial essay is twofold: to review the cross-sectional radiological anatomy and variants of the structures within the hepatoduodenal ligament, and to illustrate the non-neoplastic conditions that may arise within the hepatoduodenal ligament.

Conclusion Familiarity with these specific entities and their cross-sectional imaging findings is fundamental for a more accurate diagnosis.

Keywords Hepatoduodenal ligament · Portal vein · Common bile duct · Hepatic artery · CT · MRI

Introduction

The hepatoduodenal ligament (HDL) can be affected by a vast array of disease processes, including conditions related to the vascular structures and biliary tract it contains, furthermore by lymph node involvement due to neoplastic and non-neoplastic diseases, or it may serve as the direct route of spread for pancreatic and gastrointestinal inflammatory processes. In addition, due to the presence of lymphatics and the biliary tree, this ligament constitutes a route of spread for infections. Finally, the presence of the portal vein, the hepatic arteries and the common bile duct, makes this structure to be inevitably involved in case of hepatobiliary surgery.

While neoplasms of the liver and pancreas potentially involving the HDL have been reviewed extensively, diagnosis of non-neoplastic conditions within this structure still represents a challenge for the clinician and the surgeon. Clinical signs and symptoms of HDL disorders are frequently absent or non-specific, ranging from non-specific abdominal pain to jaundice or signs of portal hypertension. Nonetheless, imaging can help narrow the wide differential diagnosis and it is mandatory for adequate surgical planning [1–5].

In this article, we review and illustrate the normal anatomy and the important anatomical variations of the HDL, whose knowledge is necessary in case of preoperative evaluations, and the non-neoplastic conditions of the HDL and of the structures therein contained one may encounter in clinical practice. For each disease, the computed

✉ Aleksandar M. Ivanovic
alexivanovic69@yahoo.com

1 Division of Abdominal Imaging, Department of Radiology, Beth Israel Deaconess Medical Center, Harvard Medical School, Boston, MA, USA

2 Department of Diagnostic Imaging, Faculty of Medicine, Center for Radiology and MRI, Clinical Center of Serbia, Pasterova 2, Belgrade 11000, Serbia

3 Department of Radiology, Brigham and Women's Faulkner Hospital, Harvard Medical School, Boston, MA, USA

4 Present Address: Department of Radiology, Brigham and Women's Faulkner Hospital, Harvard Medical School, 75 Francis Street, Boston, MA, USA

5 Present Address: HealthAlliance-Clinton Hospital, University of Massachusetts Medical School, Leominster Campus, 60 Hospital Road, Leominster, MA, USA

tomography (CT), and magnetic resonance imaging (MRI) features are presented, with ultrasonographic correlation, when available.

Normal anatomy and anatomical variants

The HDL is a ligament that, together with the gastrohepatic ligament (GHL), forms the lesser omentum. Embryologically, it originates from the dorsal portion of the primitive ventral mesentery and extends from the flexure between the first and second portions of the duodenum to the porta hepatis. An inferior extension of the lesser omentum, containing the gallbladder neck and cystic duct are considered part of the HDL.

Together with the GHL, the HDL forms the anterior wall of the omental bursa (bursa omentalis). The lateral, free edge of the HDL serves as the anterior border of the Foramen of Winslow, which connects the lesser to the greater sac (Fig. 1) [4, 6].

The HDL connects the retroperitoneal space to the hepatic hilum, being a preferential route of spread for inflammatory, infectious, and neoplastic conditions. The dorsal portion of the primitive ventral mesentery, from which the HDL originates, is contained in the ventral anlage of the pancreas until the 8th embryonic week. Therefore, pathological processes arising in the pancreas can spread easily to the porta hepatis and liver. The portal triad, contained in HDL, may serve as a connection to the liver. Conversely, inflammatory conditions arising in the hepatobiliary structures may spread to the retroperitoneal space [6, 7].

The HDL encompasses the main portal vein, hepatic artery, common bile duct (CBD), part of the cystic duct and the gallbladder neck, lymphatics, nerves, and connective tissue [8]. The extrahepatic bile duct and proper hepatic artery are usually located anterior to the portal vein, with the artery placed to the left of the bile duct (Figs. 2, 3) [9]. In a study on 200 cadavers, however, this configuration was found in only 34.5% of cases, with most variations due to aberrant and accessory hepatic arteries [10]. Interestingly, a "normal" hepatic artery configuration was found in only 9% of cases in another study on 148 cadavers, with an artery (either an aberrant or the proper hepatic artery) running along the free edge of the HDL in 19% of cases (Fig. 4) [10, 11]. Anatomical variations of bile duct anatomy are quite common as well. For example, a low cystic

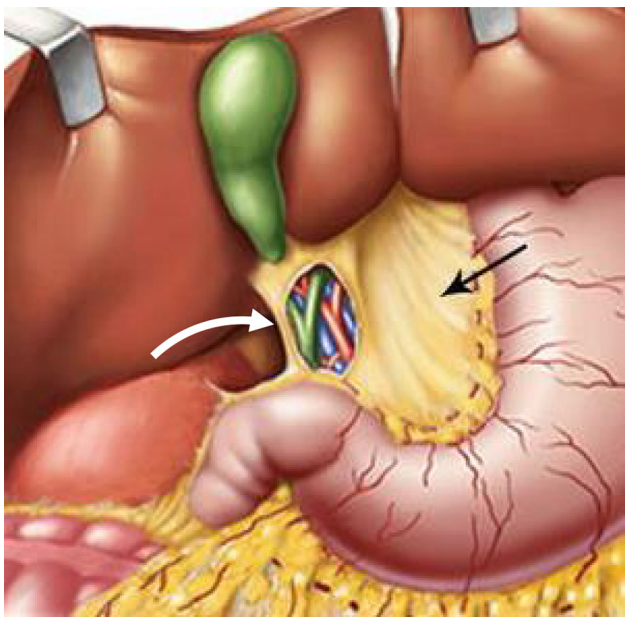

Fig. 1 Anatomy of the omental bursa and of the hepatoduodenal ligament (reproduced with permission from abdominalkey.com) showing the Winslow foramen (curved white arrow), the hepatoduodenal and the gastrohepatic ligament (black arrow). The hepatoduodenal ligament is partially opened to show its content, the common bile duct and cystic duct (green), the proper hepatic artery (red) placed to the left of the bile duct and the portal vein, located posteriorly (blue)

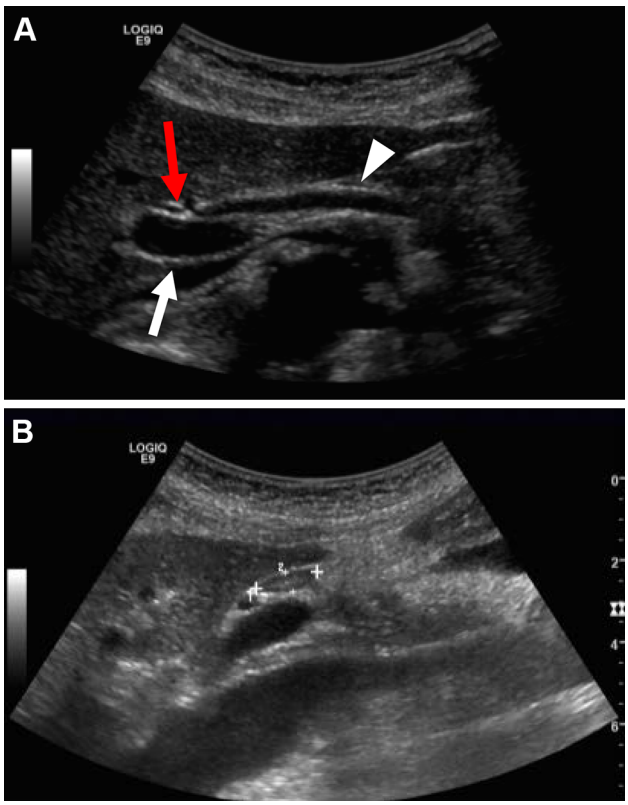

Fig. 2 Sonographic anatomy of the hepatoduodenal ligament in a 34-year-old man with mild upper abdominal discomfort. Transverse transabdominal ultrasound scan of the hepatoduodenal ligament shows the portal vein (white arrow), the common bile duct (white arrowhead) and the hepatic artery (red arrow) appearing as tubular anechoic structures in **a**. An oval, slightly hypoechoic structure representing a reactive lymph node can be demonstrated in **b**

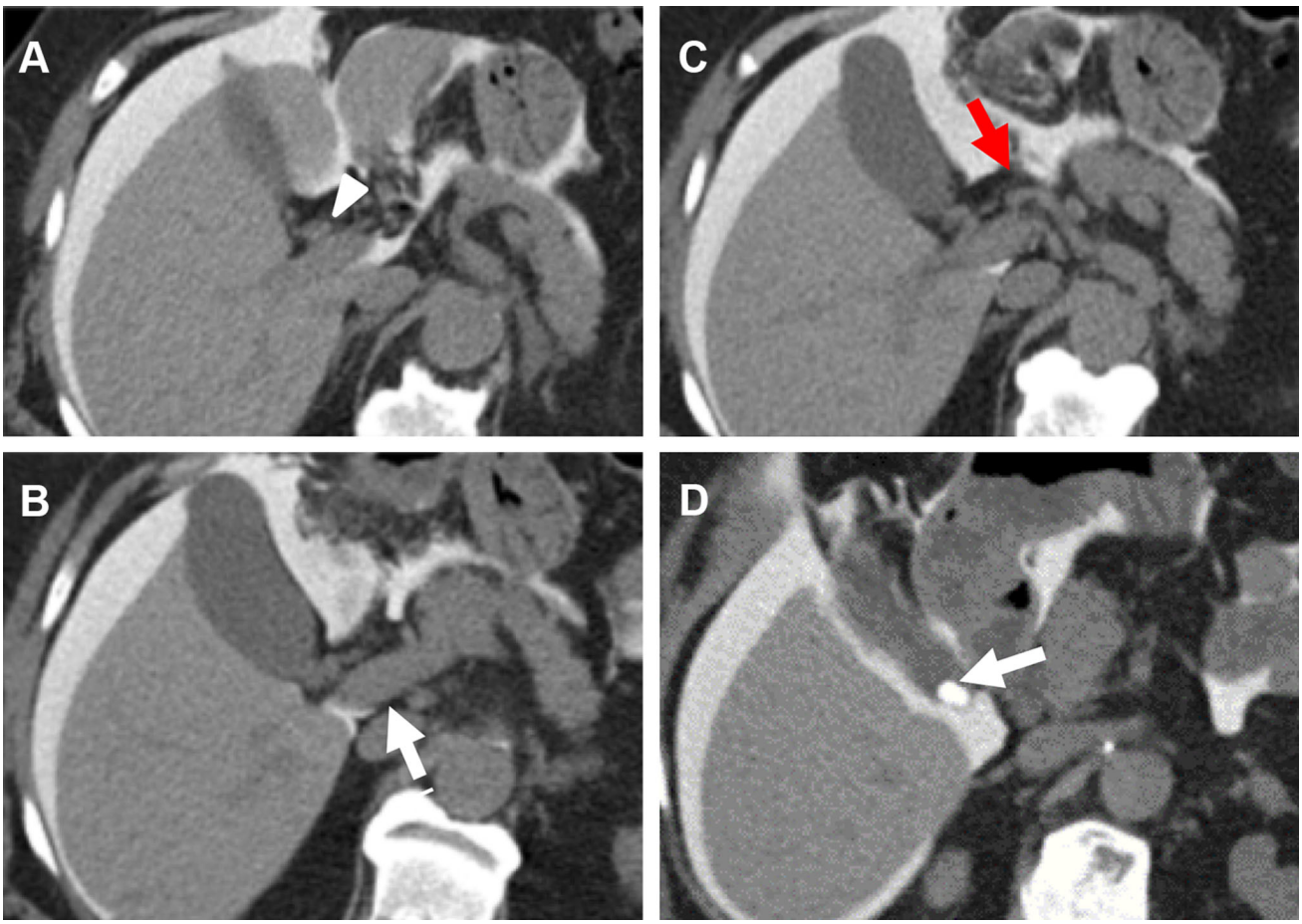

Fig. 3 Anatomy of the HDL in a 67-year-old man on peritoneal dialysis. CT peritoneography delineates the HDL and common bile duct (white arrowhead) (**a**), portal vein (white arrow) (**b**) and the hepatic artery (red arrow) (**c**). Cholelithiasis within the gallbladder neck is also demonstrated (white arrow) (**d**). Courtesy of Jennifer W Uyeda, MD; Emergency Radiology Brigham and Women's Hospital, Boston, MA; USA

duct insertion, which prevalence is estimated to be 9%, is characterized by fusion of the cystic duct with the distal third of the CBD (Fig. 5) [8, 12].

The CBD in the HDL is surrounded by the epicholedochal venous plexus of Saint, which drains into the paracholedochal venous plexus of Petren, coursing parallel to the bile ducts and draining into the hilar veins, the right gastric vein, the posterosuperior pancreaticoduodenal vein, and the superior mesenteric vein [13]. These plexuses become prominent and sometimes visible on CT or MRI in case of portal hypertension [14].

Imaging modalities and imaging anatomy

Ultrasound Transabdominal ultrasound (US) is the most widely available and inexpensive modality for the evaluation of the contents of the HDL. It allows visualization of the connective tissue, the portal vein, the hepatic artery, lymph nodes, and part of the extrahepatic bile duct [5, 15]. With the use of Doppler sonography, a precise quantification of the portal venous and hepatic arterial flow is possible, increasing the sensibility of US for detecting portal vein thrombosis, portosystemic shunting, arteriovenous shunting, and many other vascular conditions [16]. Laparoscopic and endoscopic US are even more accurate techniques, although less available and more invasive. On US, the HDL appears as a hyperechoic structure in which tubular anechoic structures, the portal vein, the hepatic artery, and the extrahepatic bile duct are contained [9, 16, 17].

Computerized Tomography (CT) is commonly performed to evaluate the structures contained in the HDL, due to its higher spatial resolution. Multiphasic contrast-enhanced CT is useful to assess both vascular anatomy and abnormalities of the structures contained in the HDL [14, 18, 19]. The hepatic artery can be correctly visualized and evaluated during the arterial phase (20 s after contrast

Fig. 4 Hepatic artery anomaly. MIP reconstructed CT image acquired during arterial phase shows an aberrant origin of the right hepatic artery from the superior mesenteric artery (arrow) and a cystic artery originating from the left hepatic artery (arrowhead), bifurcating in a deep and superficial branch

media injection) and can be studied with MPR and MIP reformatted images. The portal vein is optimally evaluated during portal venous phase (70 s after contrast media injection) [16]. The CBD appears as a hypodense tubular structure running in the HDL and can be optimally studied with MinIP reformatted images [5, 20].

Magnetic Resonance Imaging (MRI), with dedicated MRCP sequences, is the imaging modality of choice for the evaluation of HDL, the portal triad, lymph nodes, and bile ducts. The hepatic artery and portal vein appear as flow-voids on unenhanced images, while gadolinium-enhanced MRI gives information similar to contrast-enhanced CT about vessels and lesion enhancement patterns [5]. In addition, the use of a hepatospecific contrast agent may help delineate the extrahepatic bile duct and could give additional information about biliary function [21]. MRCP with 3D images allows accurate visualization of biliary structures, their normal anatomy and variations, and various pathological conditions [22, 23].

Spectrum of disorders

Lymphatics and connective tissue

Reactive lymphadenopathy

Visualization of the lymph nodes in the HDL, also called "daisy chain nodes", is not uncommon even in patients without liver disease on cross-sectional imaging (Fig. 2) [24, 25].

Enlarged lymph nodes (> 6 mm in short-axis diameter) are indicative of lymphadenopathy and should therefore be investigated. According to the appearance of lymph nodes, a differential diagnosis of underlying conditions can be suggested. Patients with cirrhosis, viral hepatitis, or other hepatic or lymphatic diseases often show enlarged hepatoduodenal nodes [26–29]. Potentially, any inflammatory condition potentially involving the mesentery could cause reactive lymphadenopathy including cholecystitis and pancreatitis, mesenteric panniculitis, primary biliary cirrhosis, and sarcoidosis [28].

In these conditions, lymph nodes are generally large (> 6 mm in short-axis diameter), or numerous, but rarely massive lymphadenopathy occur. The lymph nodes are isoechoic to the liver on US, show soft-tissue attenuation on CT, and are slightly hyperintense relative to the liver on T2-weighted MR images due to edema. These are homogeneously enhancing following intravenous contrast material administration [15, 18, 27, 28]. Differential diagnosis should be made with neoplastic adenopathy, which can appear bulky and homogeneous, or necrotic in case of metastases, infection, and high-grade lymphoma [15, 27].

Tuberculosis

Hepatoduodenal lymph nodes are a frequent site affected by tuberculous lymphadenitis. On CT, multiple enlarged lymph nodes, sometimes conglomerating with multilocular appearance and peripheral enhancement with central hypodensity are observed [30]. Other less common enhancement patterns, such as mixed and homogeneous enhancement, have been described. Lymph nodes are generally smaller than 4 cm in size. After treatment or healing, the lymph nodes can calcify. On MRI, affected nodes show central hyperintensity on T2-weighted images due to caseous necrosis and similar contrast enhancement [31, 32]. Perinodal hyperintensity on T2-weighted images, probably reflecting capsular disruption, is another reported MRI feature [33, 34]. On US, TBC nodes tend to be conglomerated with central hypoechoic areas [31].

Reactive edema

Reactive edema of the HDL can be observed in a multitude of conditions, including heart failure, liver transplant, cholecystitis, cholangitis, prior radiation therapy, or can be idiopathic. MR and CT shows edema as diffuse hypodensity of the HDL on CT and T2-weighted hyperintensity/T1-weighted hypointensity changes of the HDL (Fig. 6).

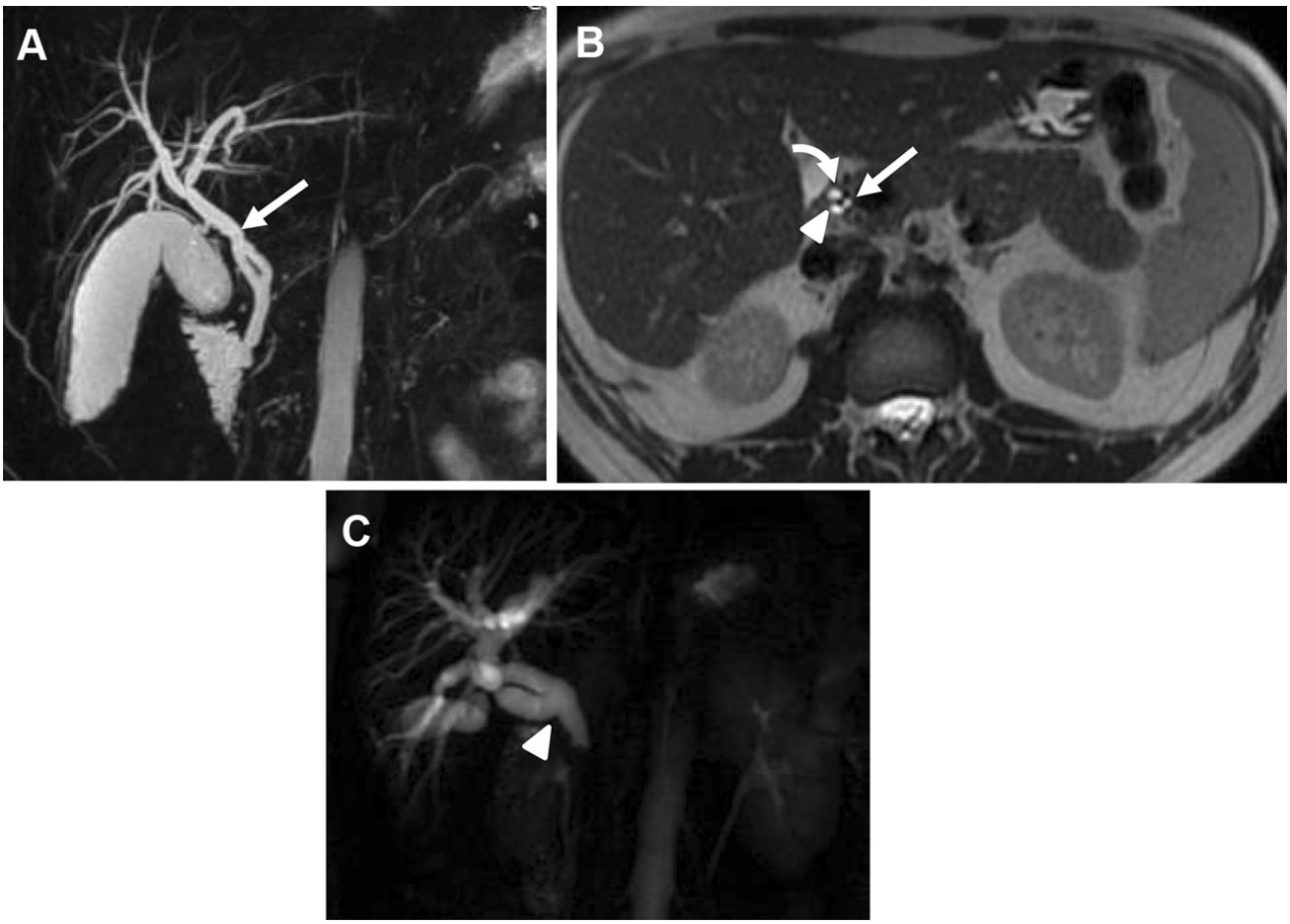

Fig. 5 Bile duct anomalies in the hepatoduodenal ligament. **a** 3D MRCP in a 89-year-old man shows low cystic duct insertion (arrow) and low bifurcation of the common bile duct. **b** T2-weighted axial image at the level of the hepatoduodenal ligament demonstrates the right (curved arrow) and left hepatic ducts (arrowhead) and the cystic duct (arrow). **c** MRCP single shot in a 38-year-old female patient with choledocholithiasis, bile duct dilatation and low bifurcation of the common bile duct (arrowhead)

Biliary tract

Choledochal cyst

Choledochal cysts are rare congenital biliary tract anomalies characterized by biliary tree dilatation. Based on the Todani classification, they can be divided in five types according to the involved part of the intra- and/or extrahepatic bile ducts [5, 35]. The type I cyst, with moderate to severe dilatation of the common bile duct without intrahepatic biliary dilatation, is the most common type and can be cystic (Ia), segmental (Ib), or diffuse fusiform (Ic). Most cysts are diagnosed in childhood, yet up to 20% manifest in adults, with female predilection. Associated conditions include liver failure, cholestasis, biliary cirrhosis, and cholangiocarcinoma (15% lifetime risk) [26, 35, 36].

The most accurate cross-sectional imaging modality for diagnosing choledochal cysts is MRCP, although MDCT with MPR reconstruction is a good alternative imaging method. Both imaging techniques provide specific information related to the location, size, and anatomic relationship of the cyst [5, 26]. MRCP or MDCT demonstrate a cystic structure or a dilation of the bile duct with biliary sludge or calculi (Fig. 7). Endoscopic retrograde cholangiopancreatography can also be used to evaluate choledochal cyst, but it is invasive and associated with complications (Fig. 7) [37].

Mirizzi syndrome

Mirizzi syndrome is a rare complication of cholelithiasis and refers to narrowing and obstruction of the CHD caused by extrinsic compression from an impacted gallstone impacted either at the gallbladder neck or in the cystic duct [23, 38]. Mirizzi syndrome could be associated with

Fig. 6 Reactive edema of the hepatoduodenal ligament. **a**, **b** 50-year-old woman with cholangiocarcinoma treated with chemotherapy and Cyberknife stereotactic radiotherapy. **a** Axial CT image obtained during early arterial phase shows hypodense material surrounding the portal vein. **b** Coronal reconstructed CT image acquired during portal venous phase demonstrates the presence of hypodense material within the hepatoduodenal ligament, consistent with post-radiation edema. **c**, **d** 47-year-old woman with weight loss. **c** Single-shot MRCP image showing fluid surrounding the common bile ducts. **d** T2-weighted coronal image demonstrate fluid within the hepatoduodenal ligament (arrows). **e**, **f** Patient with acute cholecystitis. **a** Single-shot MRCP image showing pericholecystic fluid extending at the porta hepatis. **d** T2-weighted coronal image demonstrates fluid within the hepatoduodenal ligament (arrowhead)

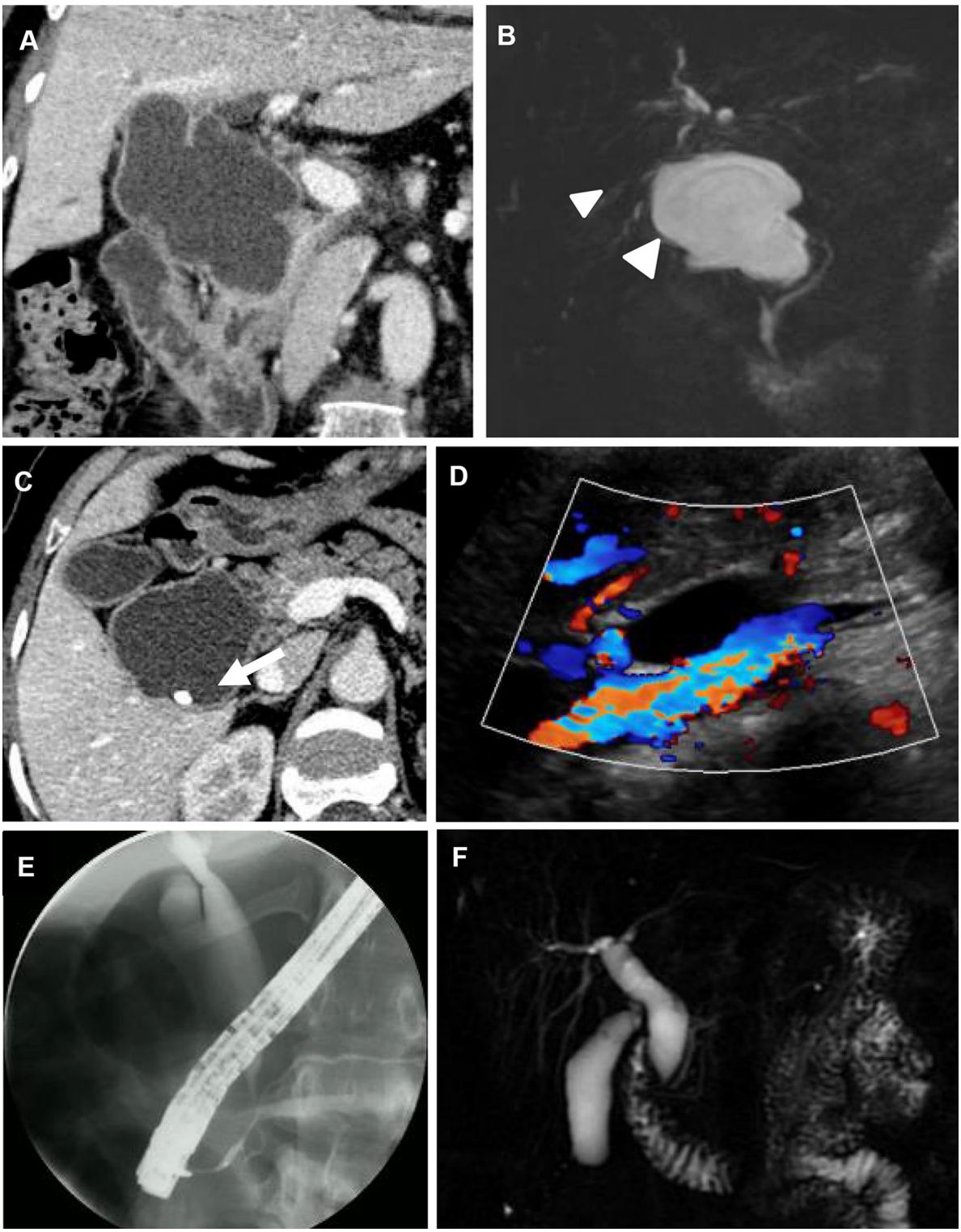

Fig. 7 Type I choledochal cyst. Coronal reformatted CT image obtained during portal venous phase (**a**) and single-shot MRCP (**b**) images in a 55-year-old man with right upper quadrant pain demonstrate fusiform enlargement of the common bile duct, with lobulated contour, consistent with choledochal cyst type Ia (white arrowheads). A small hyperdense calculus within the cyst is seen on axial CT image obtained during portal venous phase (white arrow) (**c**). **d** Transabdominal color-doppler ultrasound at the level of the hepatoduodenal ligament in a different patient shows a dilated cystic structure anterior to the portal vein. **e** Endoscopic retrograde cholangiopancreatography confirms the segmental dilation of the common bile duct (type 1b). **g** Single-shot MRCP in a different patient shows diffuse fusiform dilation of the common bile duct (type Ic)

absence (type 1) or presence of fistula (type 2-4) between the site of impaction of the gallstone and the CHD [39].

Although diagnosis of Mirizzi syndrome may be difficult with non-invasive imaging, MRCP and CT provide a correct diagnosis in most of the cases, showing cholelithiasis, stone in the cystic duct, focal narrowing of the CHD, upstream biliary dilatation and a distal CBD with normal caliber (Fig. 8). Differential diagnosis should include cholangiocarcinoma, since association between gallbladder carcinoma and Mirizzi syndrome has been reported [5, 38]. Preoperative diagnosis can be challenging: clinical evaluation of the patient may help, and elevated CA 19-9 levels are indicative of malignancy [5, 38].

Cholecysto-duodenal fistula

Bouveret's syndrome due to a cholecysto-duodenal fistula was first described in 1896 and it refers to gastric outlet obstruction secondary to impaction of a gallstone in the duodenum (or stomach). It is rare condition often seen in the elderly women [40, 41].

On CT, the impacted gallstone and the gastric outlet obstruction are seen. Multiplanar reconstruction helps evaluating the presence of cholecysto-duodenal fistula, which can occur within the boundaries of the HDL (Fig. 9). Endoscopy may serve both as a diagnostic tool and for gallstone removal [41].

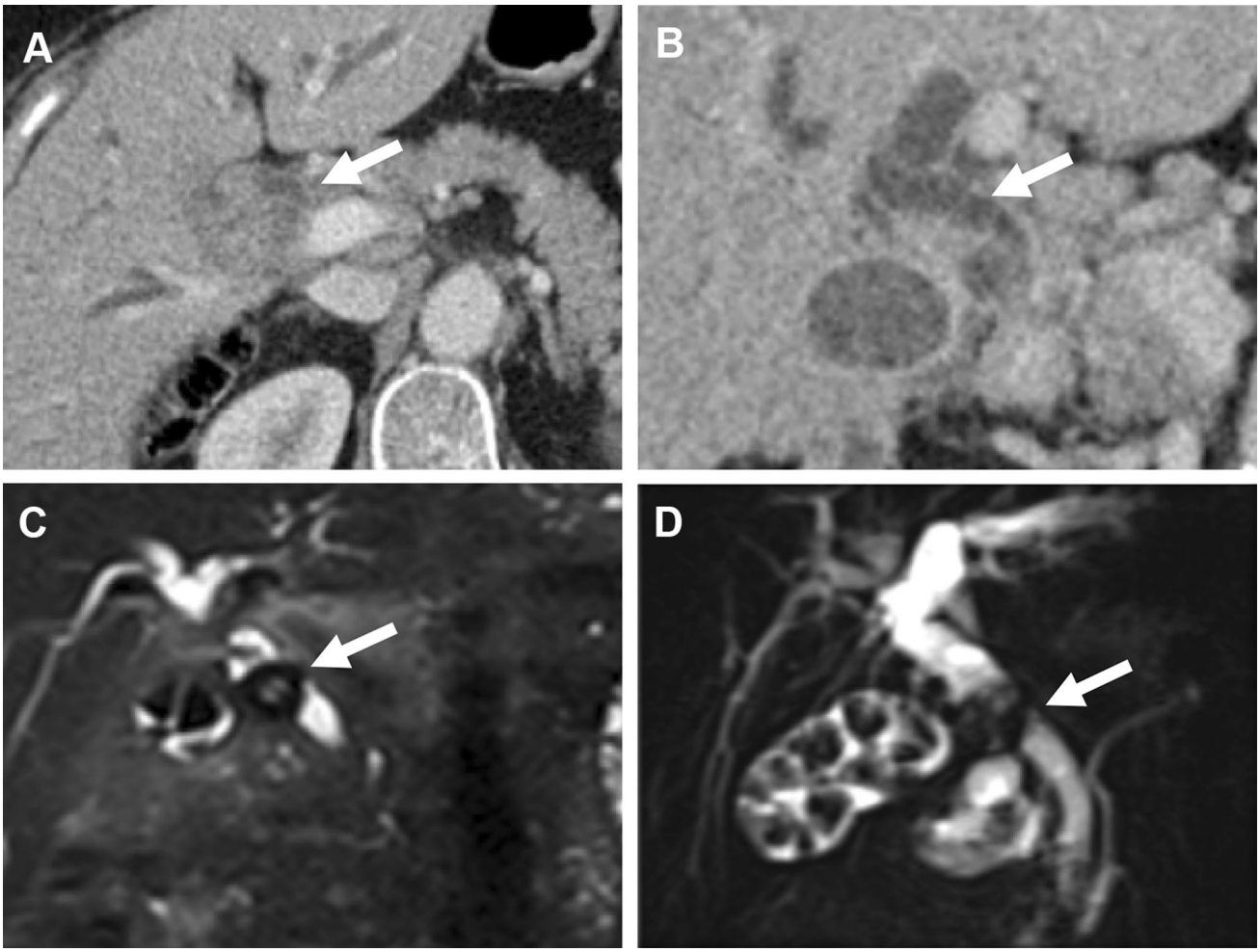

Fig. 8 Mirizzi syndrome. Contrast-enhanced axial and coronal CT images obtained during portal venous phase (**a**, **b**) and T2-weighted fat saturated coronal MR (**b**) and single-shot MRCP (**d**) images show cholelithiasis and extrinsic compression of the CBD (white arrow) by large gallstone at the level of the cystic duct, within the confines of the HDL. Moderate upstream biliary dilation is also observed. Differentiation from a cholangiocarcinoma can be difficult in (**a**)

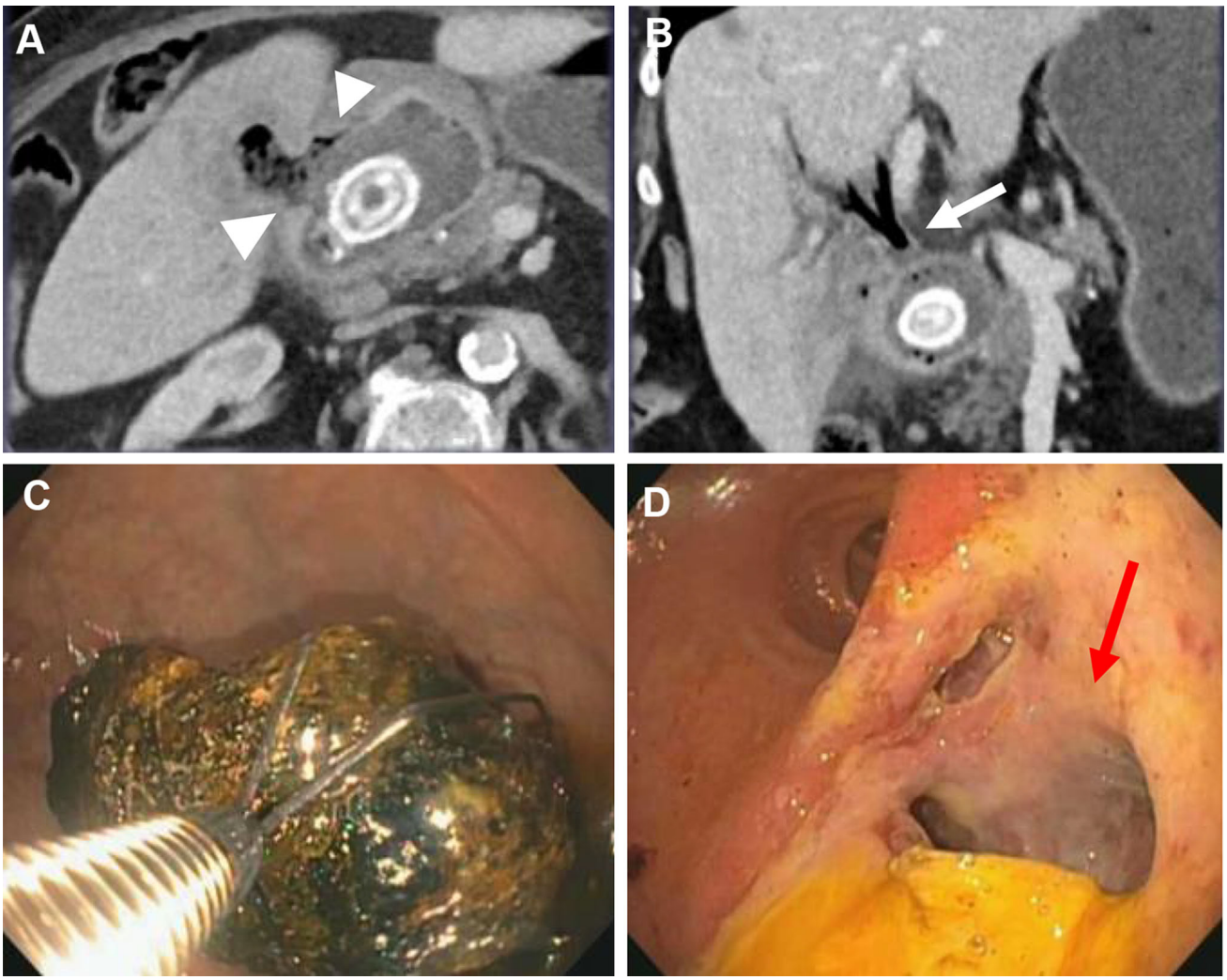

Fig. 9 Cholecysto-duodenal fistula in a 72-year-old woman with right upper quadrant pain and fever. **a** Axial contrast-enhanced CT image obtained during portal venous phase reveals a hyperdense calculus in the duodenum with a bilioenteric fistula (white arrowhead). **b** Coronal MPR reformatted image shows aerobilia (white arrow). Endoscopic image shows removal of the impacted gallstone within the duodenum (**c**), with post endoscopic removal image reveals the large cholecystoenteric fistula (red arrow) (**d**)

Portal biliopathy

Portal biliopathy refers to biliary obstruction associated with enlargement of the peribiliary collateral veins occurring in patients with portal vein occlusion or cavernous transformation of the portal vein [42]. In case of chronic portal vein occlusion, multiple venous collaterals from the plexus of Saint and Petren are recruited to compensate the diminished hepatopetal portal flow. Consequently, peribiliary venous varices may form, surrounding, scalloping, and narrowing the bile ducts [42, 43]. Three patterns of biliary involvement in portal biliopathy have been described: the varicoid pattern, with irregular contour of the bile ducts due to multiple smooth extrinsic compressions of dilated collateral veins ("the pseudocholangiocarcinoma sign"); the fibrotic pattern, with a dominant bile duct stricture, generally localized at the CBD, with proximal dilatation and the mixed pattern (Fig. 10) [44].

Most patients are asymptomatic, possibly with elevated bilirubin or alkaline phosphatase, although jaundice and right upper quadrant pain may also occur.

Contrast-enhanced CT depicts cavernous transformation of the portal vein, marked dilatation of the intra and extrahepatic portions of the peribiliary plexuses, and gallbladder varices. Coronal MPR reconstruction helps in defining bile ducts involvement, showing stenoses, fibrotic strictures, irregular and thickened wall of bile ducts [42].

MRCP is the best diagnostic tool to diagnose and depict portal biliopathy, with accuracy comparable to direct cholangiography [44]. MRCP depicts biliary wall

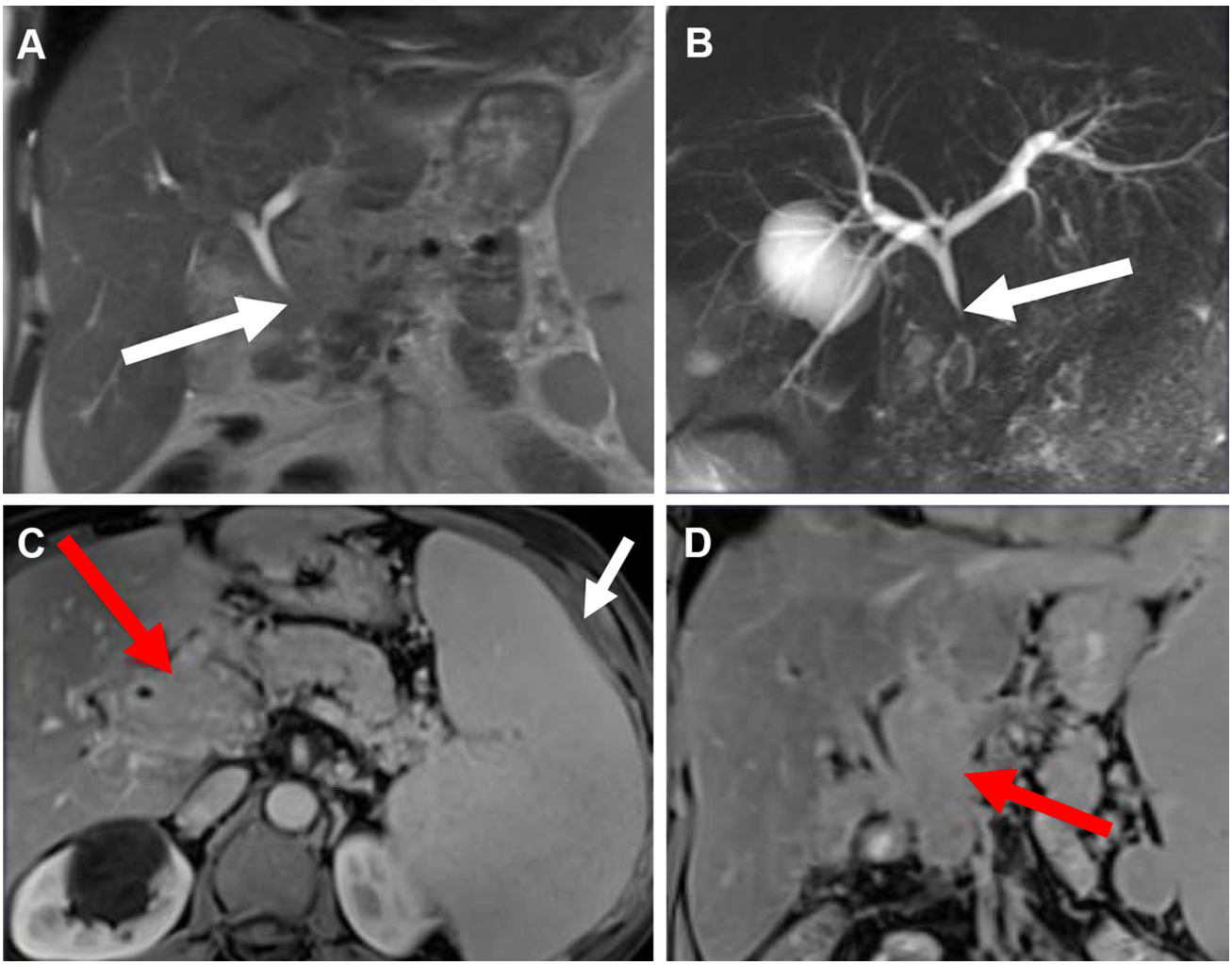

Fig. 10 Portal biliopathy in a 47-year-old male patient with increased liver function tests. **a** Coronal T2-weighted images show narrowing of the distal common bile duct (white arrow), **b** single-shot MRCP image demonstrates mild intrahepatic bile duct dilatation, with gradual narrowing of the distal CBD (white arrow). Axial (**c**) and coronal (**d**) contrast-enhanced T1-weighted images obtained during portal venous phase demonstrate varices (red arrows) surrounding the extrahepatic bile ducts, and compressing the common bile duct, findings consistent with portal biliopathy. Splenomegaly is also demonstrated (white arrow). Courtesy of Antonio Eiras-Araujo, MD; Universidade Federal do Rio de Janeiro, Rio de Janeiro, Brasil

thickening with delayed progressive enhancement on post-contrast images. In the mixed type, MRCP shows irregular contours with areas of narrowing and dilatation [44–46]. In general portal biliopathy may mimic cholangiocarcinoma: the associated vascular abnormalities may help differentiating the two [43, 44, 46].

Migrated cholecystectomy clip

Post-cholecystectomy clip migration is rare and can lead to complications which include clip-related biliary stones [47]. MRCP and CT may be useful to depict the presence of a migrated clip and associated complications. The history of previous cholecystectomy and the presence of abdominal pain, jaundice, or fever might raise suspicion for impacted migrated cholecystectomy clip. CT show the clip within the biliary tract, while MRCP is more accurate in depicting bile duct dilatation, or complications, such as cholangitis (Fig. 11) [47, 48].

Long cystic duct remnant

A long cystic duct remnant is defined as residual duct greater than 1 cm in length. It may be associated with post-cholecystectomy syndrome in presence of stones, or adhesions [49]. Rarely a cystic duct mucocele can occur, in

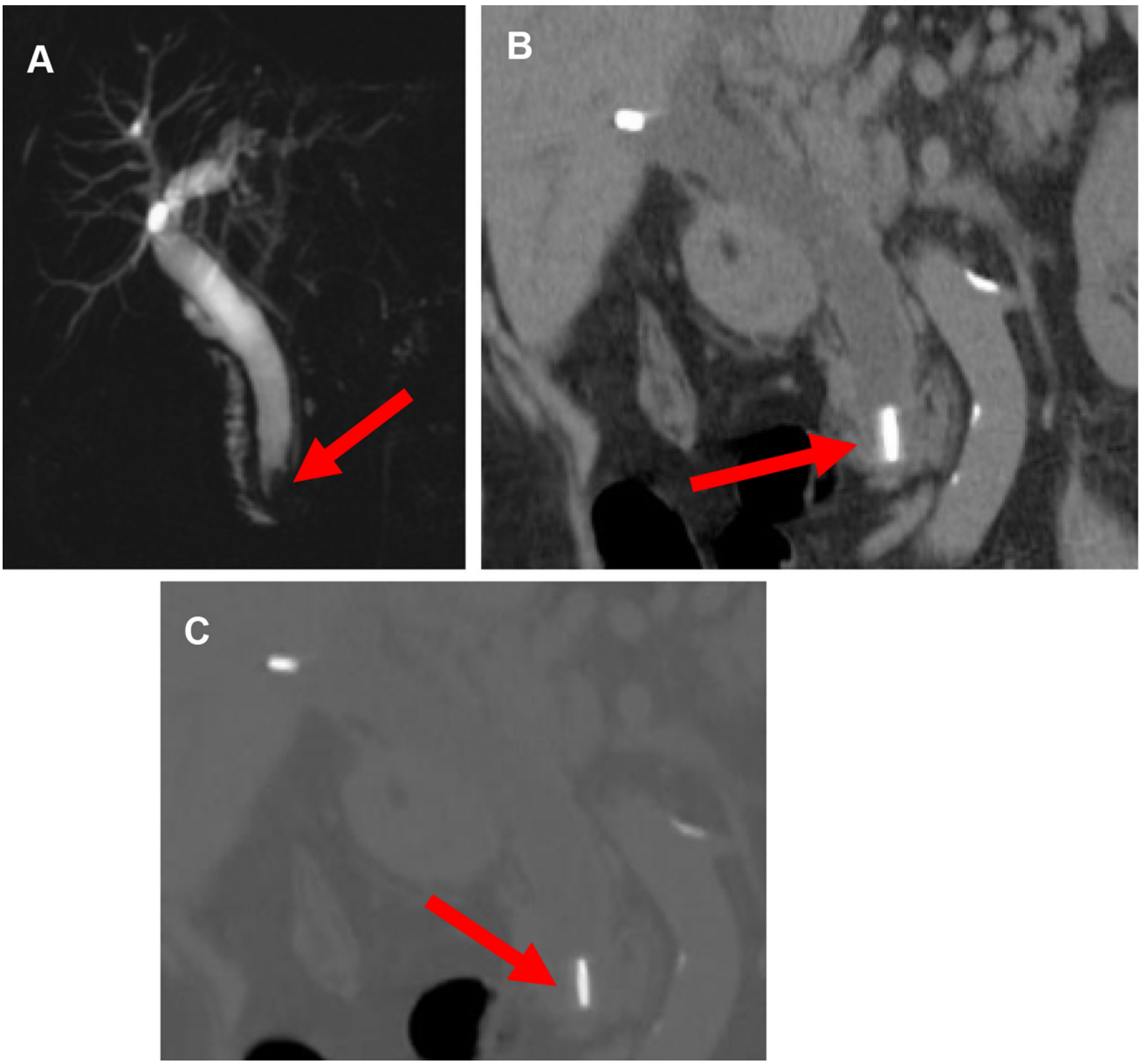

Fig. 11 Migrated cholecystectomy clip in a 50-year-old woman with history of prior cholecystectomy presenting with RUQ pain and jaundice. MRCP (**a**) and Coronal reformatted CT (**b**) images show the impacted migrated cholecystectomy clip within the distal CBD, seen as signal void in (**a**) and as a hyperdense structure in (**b**) and (**c**) (red arrow), with moderate intra and extrahepatic bile duct dilatation

which the remnant becomes distended with mucus. Cholangiography, CT, or MRCP demonstrate a dilated cystic duct, sometimes with sludge, microcalculi and inflammatory changes [50].

Benign biliary stricture

Postsurgical biliary stricture represents the most common cause of benign biliary stricture occurring in 0.6% of cases after cholecystectomy. Most commonly, post-cholecystectomy strictures are located at the junction of cystic duct and CBD or at the hepatic confluence. Unrecognized anatomical variants, inflammation and inadvertent ligation of the cystic duct close to its insertion are the main risk factors [23, 51].

MRCP shows location of the stricture and the presence of biliary dilatation. MRCP, however, tends to overestimate the length of the stricture, especially when the CBD is collapsed distally to the stricture [51].

Biliary strictures after liver transplant could be divided into anastomotic and non-anastomotic types. Anastomotic strictures are due to fibrosis and scars, and they appear as single, short-segment strictures localized at the level of the anastomosis on MRCP (Fig. 11) [51]. Non-anastomotic

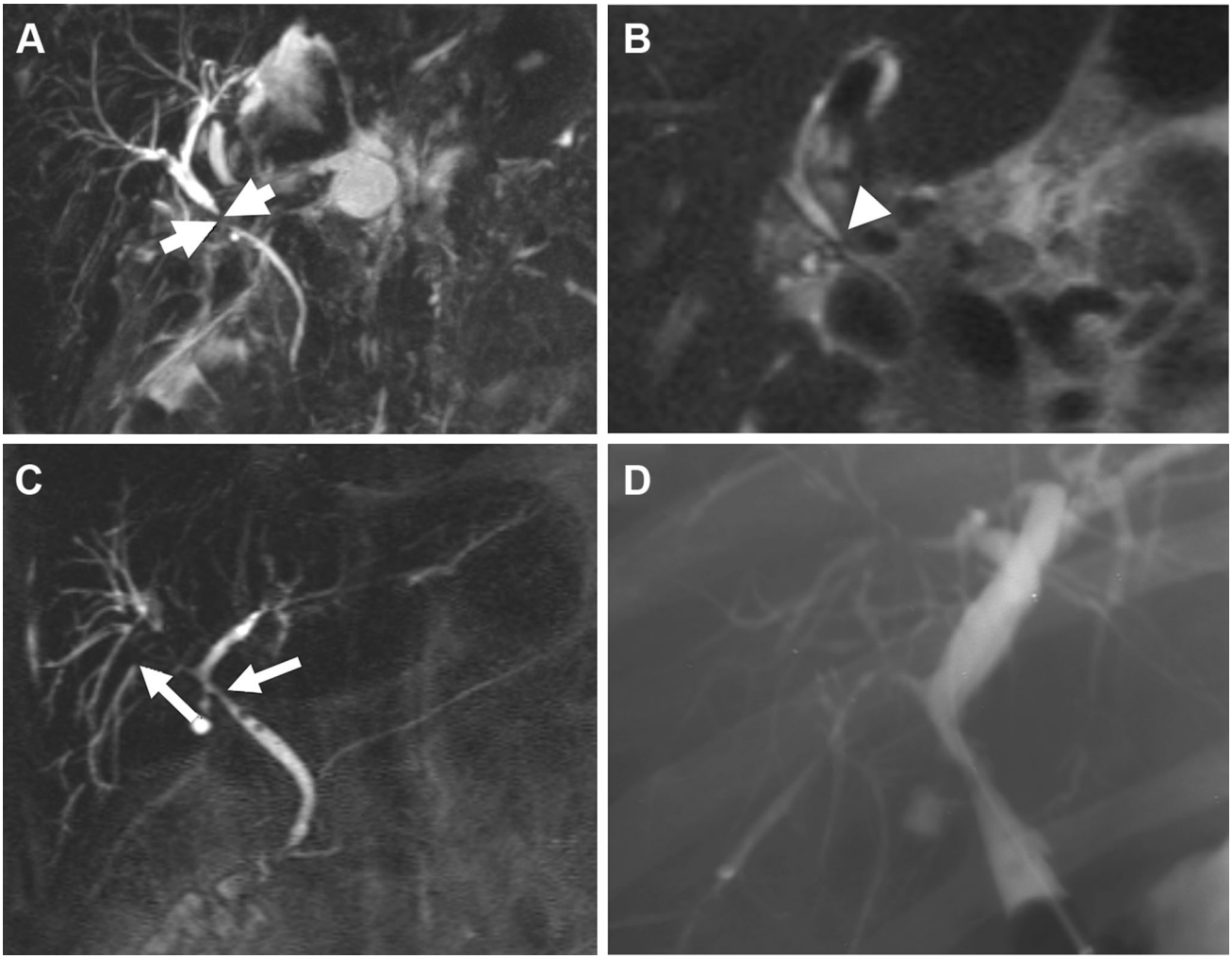

Fig. 12 Benign biliary strictures. **a** 3D MRCP image in a patient with orthotopic liver transplantation shows a focal stricture at the common bile duct (arrows). **b** Coronal T2 weighted image confirm the stenosis at the level of the anastomosis (arrowhead). **c** Single-shot MRCP image in a different patient with orthotopic liver transplantation shows multiple strictures throughout the biliary tree (arrows), confirmed on endoscopic retrograde cholangiopancreatography (**d**), consistent with non-anastomotic strictures

strictures develop secondary to ischemic or immunologic causes. MR cholangiopancreatography shows multiple stenosis involving the intrahepatic ducts, the hepatic hilum, and the CHD (Fig. 12) [51, 53].

Bile leak

A bile leak could form after an injury to any bile duct, commonly from cystic duct injury after cholecystectomy, or from CBD or intrahepatic bile duct injury after liver transplantation. MRCP with the use of hepatospecific contrast media can be particularly useful differentiating bile duct leak from other postoperative fluid collection. MRCP shows a T2-weighted hyperintense fluid collection connected to the biliary tree, and accumulation of contrast within the lesion can be observed on hepatobiliary phase [54, 55].

Ischemic cholangiopathy

Ischemic cholangiopathy refers to the focal or extensive damage to the bile ducts due to impaired blood supply to the bile ducts. This can occur as the terminal event of a vast array of conditions injuring the peribiliary vascular plexus, a group of arterioles and capillaries arising from hepatic artery, including liver transplant, vasculitis, radiation, and hepatic artery chemoembolization [52].

On US dilated bile ducts and bilomas throughout the course of the biliary tree can be appreciated [53]. MRCP may also show debris within the dilated bile ducts (Fig. 13) [53].

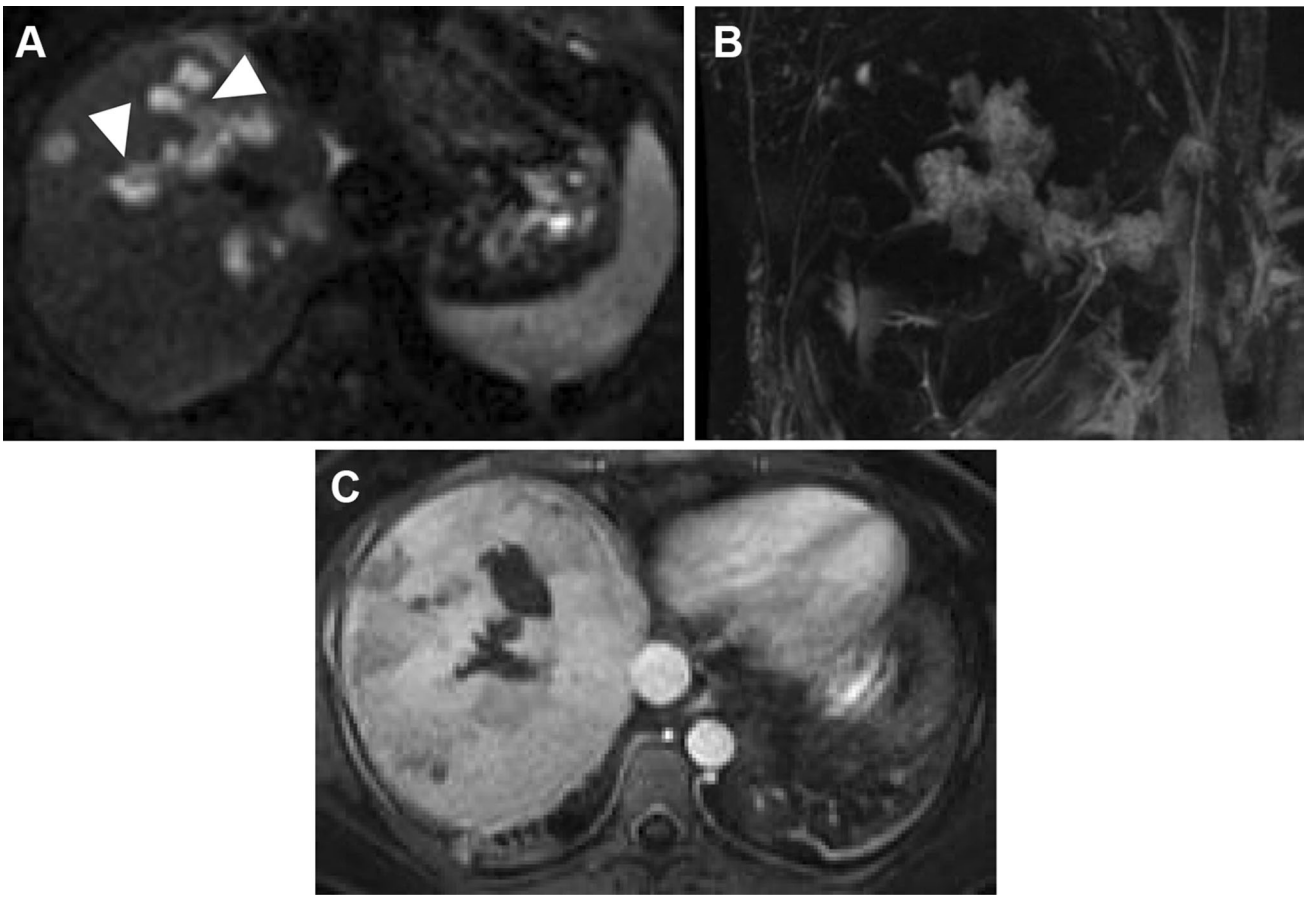

Fig. 13 Ischemic cholangiopathy in a patient with orthotopic liver transplantation. **a** Diffusion weighted image shows dilated intrahepatic bile ducts with T2 hypointense debris within their lumen (arrowheads). **b** 3D MRCP shows diffuse dilation of the biliary tree extending at the porta hepatis. **c** Contrast-enhanced axial T1-weighted fat suppressed image acquired during arterial phase shows heterogeneous enhancement of the liver suggesting altered hepatic arterial flow

Acute ascending cholangitis

Acute ascending cholangitis is a potentially life-threatening disease caused by bacterial overgrowth and infection. Clinically, it manifests with the Charcot triad (fever, jaundice and abdominal pain), although clinical presentation may be subtle, especially in elderly or immunocompromised patients [56]. It is almost invariably associated with biliary obstruction and increased biliary pressure. Other causes are iatrogenic, occurring in 18% of transhepatic percutaneous biliary drainage catheter placements, related to sclerosing cholangitis or parasitic infections [56, 57].

Complications include sepsis, hepatic abscesses, portal vein thrombosis, and peritonitis in the acute setting; biliary stricture and cholangiocarcinoma when chronic.

The most common imaging signs of acute cholangitis are biliary obstruction with intra- and extrahepatic biliary duct dilatation (depending on the cause of obstruction), diffuse and concentric thickening of the biliary wall. Hyperenhancement of biliary walls and pneumobilia can also be observed. MRCP better depict biliary dilatation, the presence of pus in the biliary tract and the nature of biliary obstruction [56].

Ascariasis

Ascaris lumbricoides is the most common helminthic infestation affecting human race, infesting 25% of the world population [56, 58]. In the HDL ascaridiasis involves biliary tract. Biliary ascaridiasis is generally asymptomatic, however can be complicated by recurrent pyogenic cholangitis, cholecystitis, pancreatitis, hepatic abscesses, and septicemia can be seen [58, 59]. Ultrasonography is safe and accurate to diagnose biliary ascaridiasis, correctly identifying more than 85% of patients with this condition. Reported sonographic findings of biliary ascaridiasis are: dilatation of bile duct, with moving long, linear or curved echogenic structures in bile duct, a distended and edematous gallbladder and liver abscesses [60, 61]. On CT, the worms are hyperattenuating relative to bile and on MR they show low signal intensity on T2-weighted images, although

the fluid-filled digestive tract of the worm is hyperintense on T2-weighted images [59, 60].

Biliary echinococcosis

Hydatid cysts are the manifestation of infection from the cestodes *Echinococcus granulosus* or *E. multilocularis*. While *E. granulosus* is found in regions around the Mediterranean Sea, south America and Oceania, *E. multilocularis* is more common in the arctic area, in northern Europe and Asia. Clinical symptoms, including abdominal pain or the presence of a mass, are non-specific and serology has a limited role, thus diagnosis relies on imaging [62, 63]. Hydatid cysts form when humans ingest echinococcus eggs, after the larvae have migrated from the intestines to other organs, such as the liver, spleen, and lungs, where they form the cysts. Imaging features of *E. granulosus* vary according to the stage of cyst development: while in the early stages *Echinococcus* cysts have the appearance of simple cysts, later, after daughter cysts develop, multiseptated wheel-like structures are seen. After the parasite dies, the septa disappear, and wall calcification may be demonstrated. US, CT, and MRCP findings reflect the stage of the cysts. In the context of biliary echinococcosis, bile duct dilation with an irregular, leaf-like appearing filling defect in the biliary tree, due to the presence of daughter cysts or hydatid membranes, can be observed, sometimes with associated cystobiliary fistulas (Fig. 14) [62, 63].

Hepatobiliary tuberculosis

Hepatobiliary tuberculosis is extremely rare, and imaging features are non-specific: cholecystitis, gallbladder mass, haemobilia, or obstructive jaundice with or without periportal mass have been described (Fig. 15). Stenosis of the biliary tree can occur due to extrinsic compression related to enlarged lymph nodes or due to inflammatory stricture, most commonly multiple. Signs of hepatic involvement, such as hepatic abscess, narrow the differential diagnosis [33, 64].

AIDS cholangiopathy

AIDS cholangiopathy, the most common AIDS-related disease involving structures in the HDL, is a form of sclerosing cholangitis occurring in patients with a CD4 count of less than 100/mm^3 [65]. Cytomegalovirus and cryptosporidia have been advocated as the main etiologic agents. Clinical symptoms are non-specific, although the presence of right upper quadrant pain and elevated cholestatic enzyme elevation in patient with low CD4 count should raise suspicion [23, 66].

US allows detection of dilated intrahepatic and extrahepatic bile duct [66]. MRCP is the most accurate modality to diagnose HIV cholangitis showing multiple intra- and extrahepatic biliary strictures and dilatation, with a beaded appearance. Other signs are wall thickening and hyperenhancement of the bile ducts, papillary stenosis, present in 75% of the cases, dilated CBD, presence of a 1–2 cm extrahepatic bile duct stricture, and acalculous cholecystitis [23, 56, 66]. Contrast-enhanced MDCT may help assessing associated liver or vascular involvement [66].

Portal venous disorders

Portal vein thrombosis is associated with a myriad of conditions, ranging from cirrhotic liver disease, pancreatitis, cholangitis, hypercoagulable states, and embolism from thrombus located in the superior mesenteric or splenic vein [67].

US, the imaging modality of choice, shows dilated portal vein (greater than 13–15 mm), and absence of variation in portal vein diameter during respirations. While an acute thrombus can appear anechoic on B-mode US and thus may not be visualized, a chronic thrombus tends to be more echogenic, and sometimes calcifications can be seen. US-Doppler can help distinguishing bland from malignant thrombosis, since the latter may show pulsatile flow in the portal vein, an extremely specific sign for this condition [18, 68, 69].

On CT, acute thrombus is generally hyperdense and tends to become isodense in chronic thrombosis. Post-contrast images can be useful to differentiate bland from tumor thrombus, since in the latter streaky enhancement can be demonstrated [16, 18, 68]. On MRI, a bland thrombus shows typically normal portal vein caliber and low T2-weighted signal intensity, while a malignant thrombus shows increased portal caliber and intermediate to high T2-weighted signal intensity (Fig. 16) [5, 68, 69]. Pylephlebitis, an inflammatory thrombosis of the portal vein, occuring as a complication of intra-abdominal infections, shows diffuse periportal edema, and can be associated with liver abscesses (Fig. 17).

Cavernous transformation of the portal vein occurs in case of portal vein obstruction and is represented by a mass-like conglomerate of tortuous vessels at the porta hepatis, in the HDL or sometimes within the liver, which can be demonstrated on US-Doppler, CT, or MRI (Fig. 18) [68, 69].

Portal vein stenosis occurs in 1% of liver recipient after liver transplantation [70]. Other causes are malignancy or

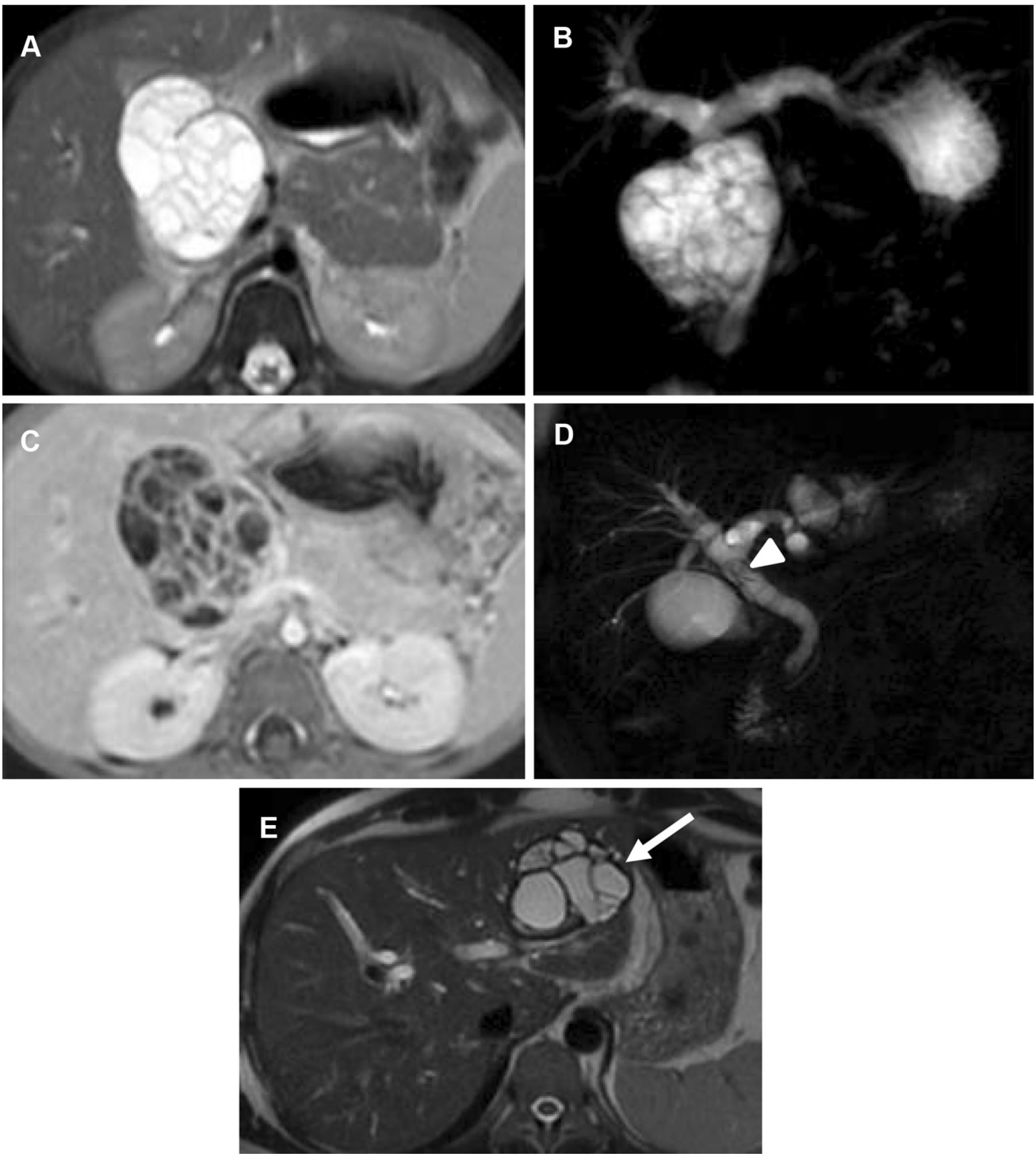

Fig. 14 Biliary echinococcosis. Axial T2-weighted image (**a**) MRCP single-shot (**b**) and axial contrast-enhanced T1-weighted during portal venous phase (**c**) in a 79-year-old man with jaundice and right upper quadrant pain show moderate intrahepatic bile duct dilatation and fusiform enlargement of the CBD, associated with multiple internal enhancing septations, representing daughter cysts in the context of echinococcal disease. Courtesy of Antonio Eiras-Araujo, MD; Universidade Federal do Rio de Janeiro, Rio de Janeiro, Brasil. **d** MRCP single-shot in a 42-year man shows a hypointense line in the common bile duct, representing a ruptured endocyst (arrowhead). **e** T2 axial image shows an echinococcal cyst in segment II and III in the same patient (arrow)

Fig. 15 Biliary tuberculosis in a 28-year-old man presenting with right upper quadrant pain. Contrast-enhanced axial CT images obtained during portal venous phase show mild inflammatory changes involving the gallbladder neck (**a**), the cystic duct (**b**), and moderate splenomegaly (**c**) (white arrows), non-specific sign of biliary tuberculosis

any surgical procedure involving resection and re-anastomosis of the portal vein [5]. Focal narrowing of portal vein and signs of portal hypertension, such as increased collateral vessels, can be appreciated on CT or MR, while US-Doppler shows a three to fourfold increased velocity across the anastomosis (Fig. 19) [5, 16].

Portal vein aneurysms are defined as focal dilatation of the portal venous system with a diameter greater than 2 cm for the extrahepatic portal vein. They are most commonly fusiform, although they can be saccular or bilobed (Fig. 20). They represent 3% of all venous aneurysms but are the most common visceral venous aneurysms. They can be congenital or acquired, due to trauma, cirrhosis, portal hypertension, surgery, and pancreatitis [5, 69, 71, 72].

Portal venous gas can be associated with various conditions, including ischemic bowel disease, bowel obstruction, ingestion of caustic substances, intra-abdominal abscesses, necrotizing pancreatitis, trauma, liver transplantation, or abdominal surgery [5, 73]. US shows reverberation artifacts along the portal vein. CT demonstrate air in the main portal vein or in its branches, which can be seen as susceptibility artifacts on MR, better appreciated on gradient echo images [5].

Conditions involving the hepatic artery

The hepatic artery can be affected by various conditions: thrombosis, stenosis, pseudoaneurysm and aneurysm formation.

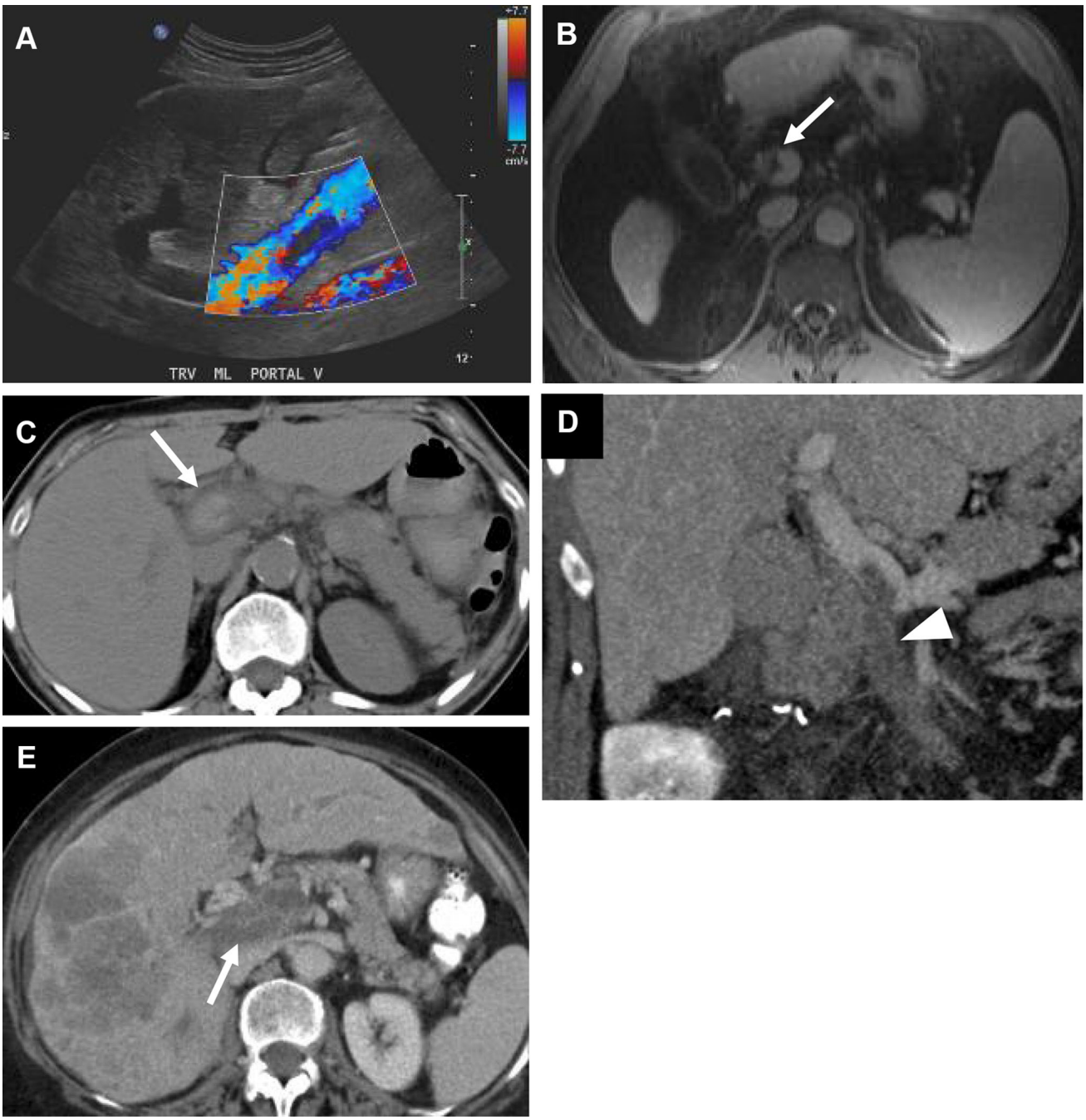

Fig. 16 Portal vein thrombosis. **a** Transabdominal color-doppler US of the abdomen shows a hypoechoic non-occluding filling defect in the portal vein, confirmed on contrast-enhacend axial T1-weighed acquired during portal venous phase (**b**) (arrow). **c** Axial CT of the abdomen in a different patient shows a hyperdense filling defect in the lumen of a dilated portal vein, representing an acute thrombus. **d** Coronal reconstructed contrast-enhanced CT acquired duding portal venous phase in a different patient shows a hypodense thrombus in the superior mesenteric vein extending into the proximal portal vein, likely representing a bland thrombus. The superior mesenteric vein shows adjacent haziness, suggesting acute thrombosis. **e** Axial contrast-enhanced CT acquired duding portal venous phase in a different patient shows a hypodense filling defect in a dilated portal vein with areas of streaky enhancement (arrow), suggesting tumor thrombosis

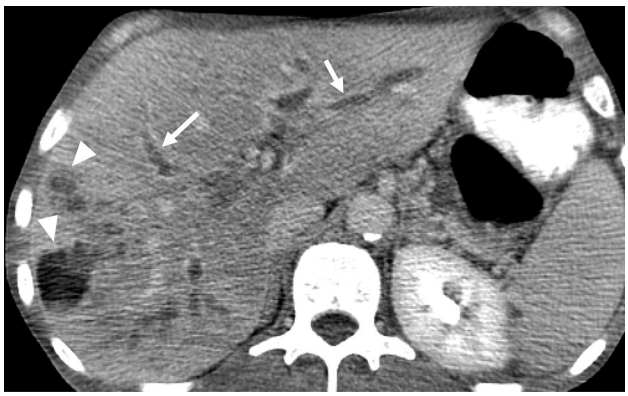

Fig. 17 Pylephlebitis. Contrast-enhanced axial CT image acquired during portal venous phase shows diffuse dilation and haziness of the hypodense portal venous branches (arrows). Focal hypodensities in the liver are also demonstrated, representing liver abscesses (arrowheads)

While the first three conditions are related to liver transplant or liver surgery involving resection and anastomosis of the hepatic artery, aneurysms can occur due to a variety of cases, including atherosclerosis, fibromuscular dysplasia, collagen vascular disease, trauma, infections, pancreatitis, and vasculitis, generally when multiple [5]. Hepatic artery thrombosis presents with absence of flow on US-Doppler and can be confirmed with contrast-enhanced CT or MR as a hypodense or hypointense filling defect within the vessel during the arterial phase. Hepatic artery stenosis show increased arterial flow at the site of stenosis, with post stenotic turbulent flow on US-Doppler, while angiographic techniques show a reduced caliber of the vessel, generally occurring at the site of anastomosis (Fig. 21) [70]. Pseudoaneurysms appear as a cystic structure with turbulent arterial flow located around the artery

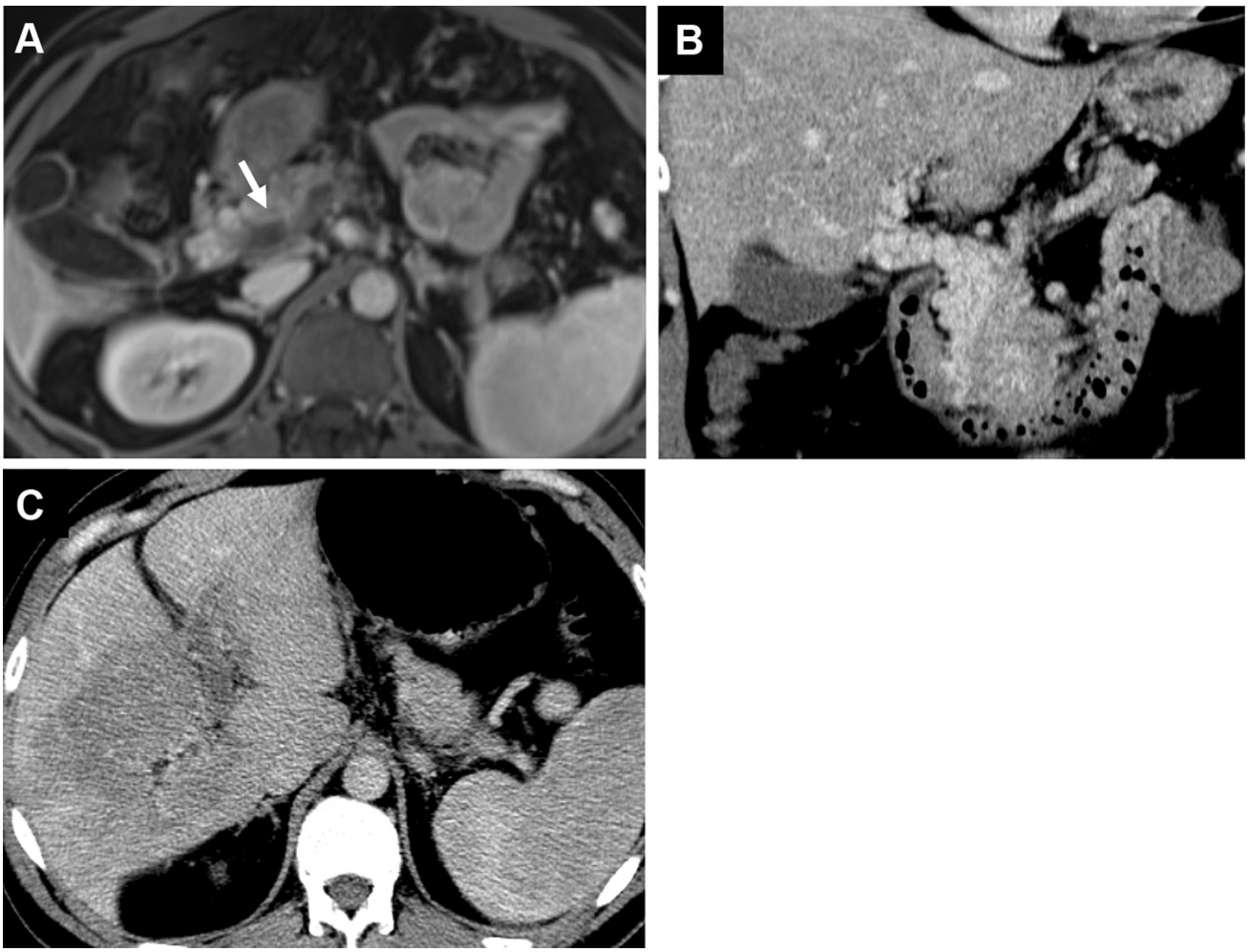

Fig. 18 Cavernous transformation of the portal vein. **a** T1-weighted fat saturated image acquired during portal venous phase shows a filling defect in the main portal vein surrounded by prominent tortuous venous collaterals (arrow). **b** Coronal reconstructed CT image acquired during portal venous phase shows a mass-like conglomerate of tortuous vessels in the HDL surrounding the portal vein. **c** Axial CT image acquired during portal venous phase in the same patient 2 years before cavernous transformation occurred, shows a hypodense filling defect in the portal vein consistent with a bland thrombus

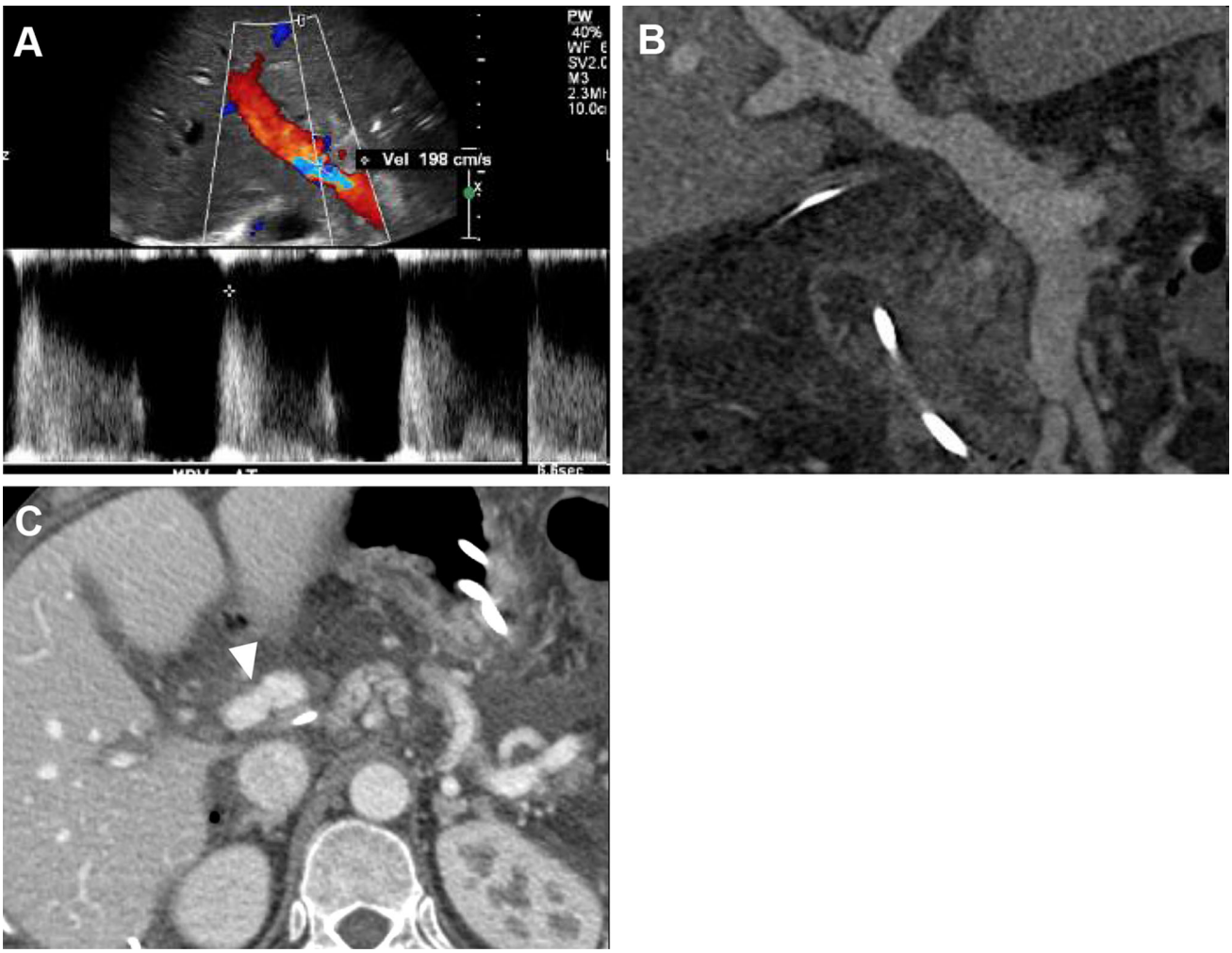

Fig. 19 Portal vein stenosis in a patient with ortothopic liver transplantation. **a** US-Doppler image shows high velocity across the anastomosis and an area of aliasing on color-doppler image at the portal vein. **b** Coronal reconstructed and axial **c** CT images demonstrate the stenosis of the portal vein occurring at the anastomosis (arrowhead)

on US-Doppler. On contrast-enhanced CT and at MR, the pseudoaneurysm enhances on arterial phase imaging (Fig. 22) [5]. Aneurysms can be diagnosed on cross-sectional images as a dilation of the artery, with turbulent flow or "yin-yang" appearance on US color-Doppler (Fig. 23) [74].

Pancreatic disorders involving the HDL

Groove pancreatitis

Groove pancreatitis is an uncommon but distinctive form of segmental pancreatitis affecting the pancreaticoduodenal groove, a region located between the head of the pancreas, the duodenum and the HDL [75]. The pathogenesis is unclear, although a strong association with history of alcohol abuse exists. Other predisposing conditions include male gender, Brunner gland hyperplasia, and dorsal dominant drainage of the pancreas. The clinical presentation varies greatly, ranging from signs of acute pancreatitis to more chronic forms [76].

Two forms of groove pancreatitis exist: a pure form, affecting only the pancreaticoduodenal groove, and a segmental form which extends into the pancreatic head [76].

CT and MRCP can be useful in diagnosing groove pancreatitis, the pure form showing fat stranding and inflammatory changes in the groove or a soft tissue mass, often with "sheetlike" curvilinear crescentic shape with increasing delayed enhancement. The segmental form shows the presence of a mass in the groove, and it is generally indistinguishable from a pancreatic head tumor. Other signs are cystic duodenal thickening, narrowing of the CBD and the MPD, pancreatic calcifications, ductal dilation, and ductal beading or irregularity [76–78].

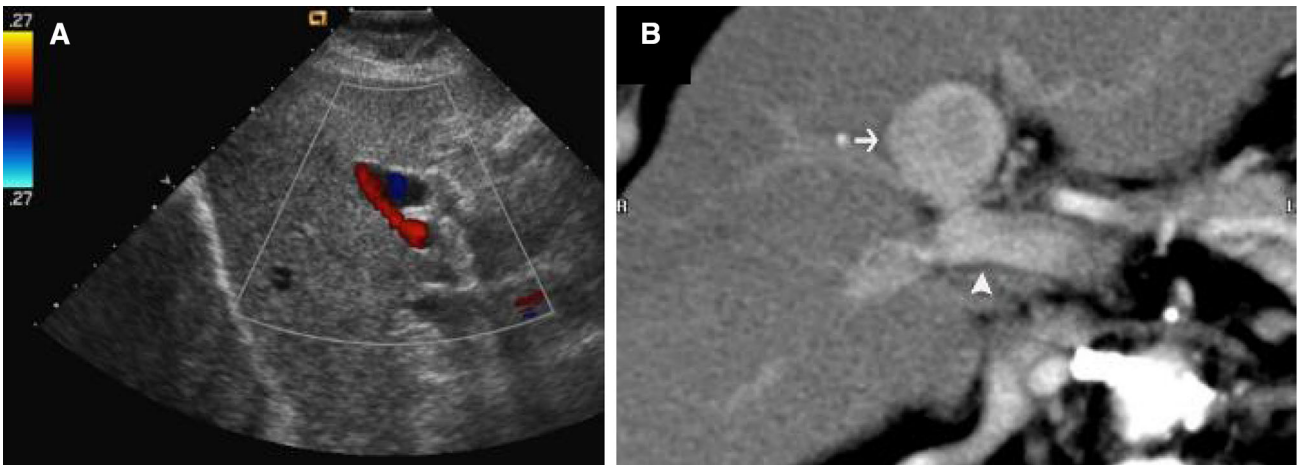

Fig. 20 Portal vein aneurysm. **a** Transabdominal color-Doppler ultrasound image shows a saccular dilation of the main portal vein with turbulent flow. **b** Axial CT image acquired during portal venous phase confirms the saccular aneurysm (arrow) of the portal vein (arrowhead)

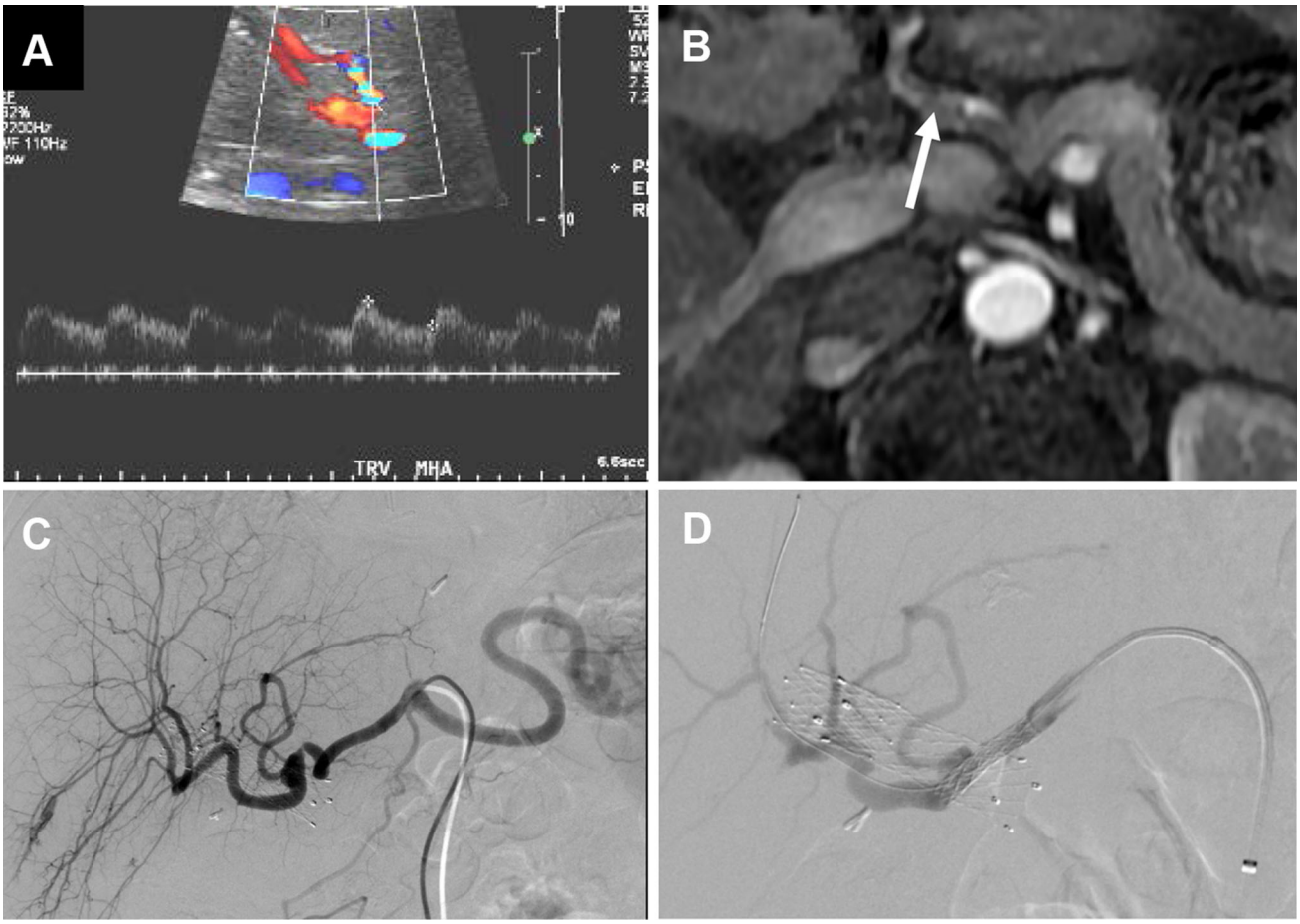

Fig. 21 Hepatic artery stenosis. **a** Transabdominal US-Doppler image of the hepatic artery shows elevated systolic and diastolic flow with aliasing. **b** Axial T1-weighted fat saturated image acquired during arterial phase shows the stenosis of the hepatic artery (arrow). Digital subtraction angiography images before (**a**) and after stent placement (**b**) confirm the stenosis of the hepatic artery

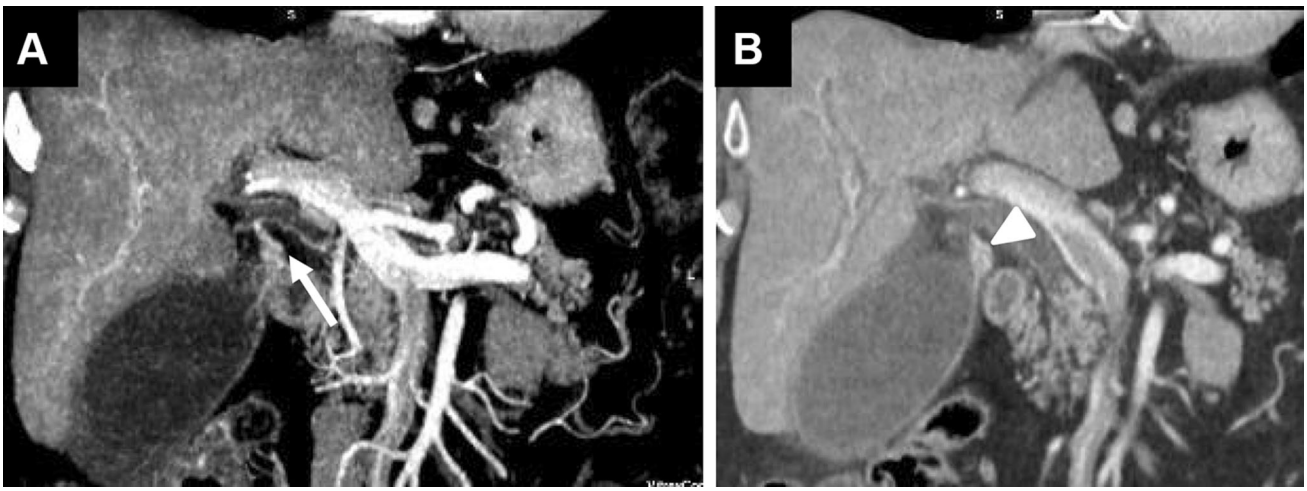

Fig. 22 Cystic artery pseudoaneurysm in patient with acute cholecystitis. **a** MIP reconstructed CT image acquired during arterial phase shows an enhancing structure (arrow) arising from the cystic artery. **b** Coronal CT reconstructed image acquired during arterial phase shows an arterially enhancing cystic structure adjacent to the gallbladder (arrowhead), which shows mild wall thickening, and adjacent fat stranding. Pseudoaneurysm of the cystic artery can occur as rare complication of acute cholecystitis. Courtesy of Dragan Vasin, MD; Department of Diagnostic Imaging, Clinical Center of Serbia, Belgrade, Serbia

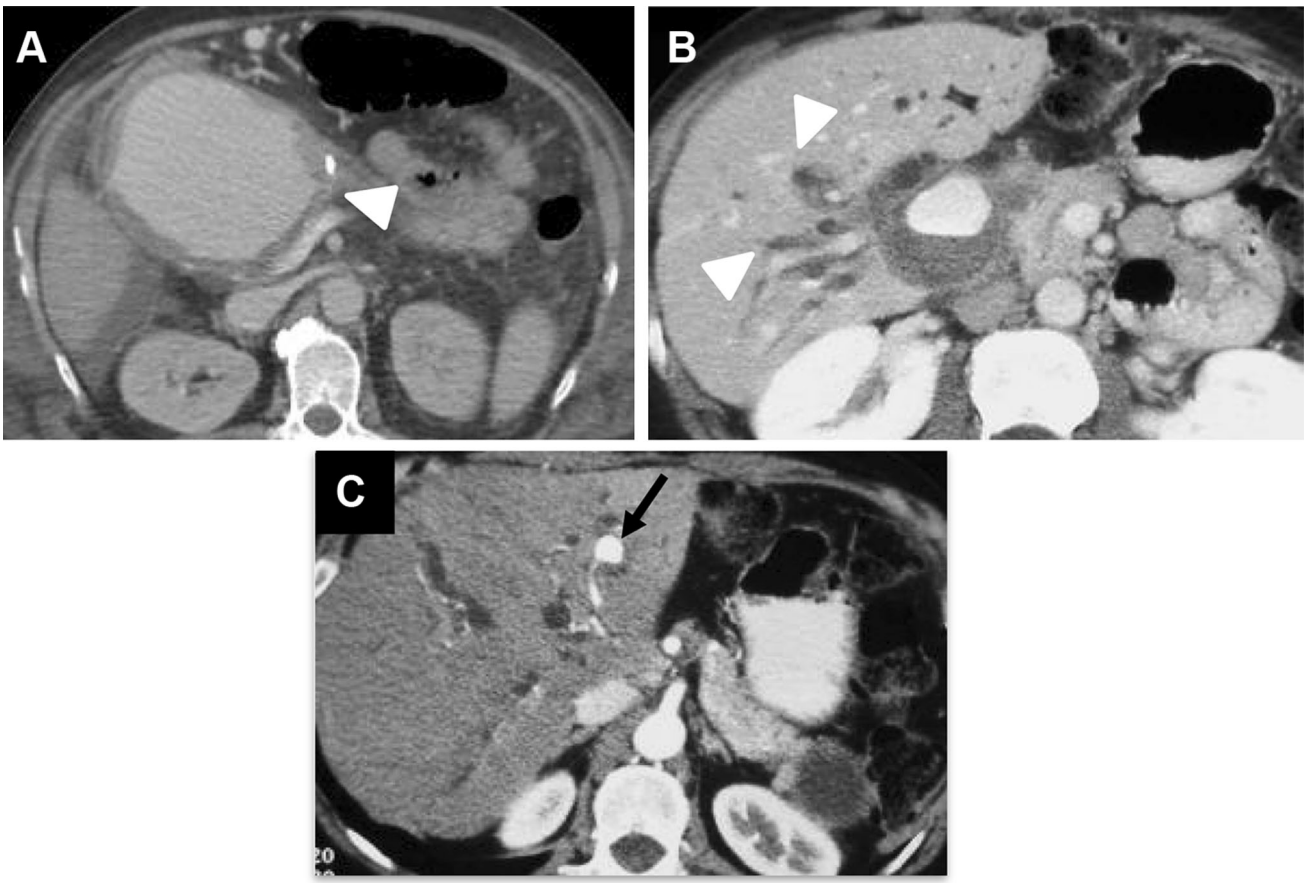

Fig. 23 Hepatic artery aneurysm in patient with cirrhotic liver disease and variceal bleeding presenting with hemorrhagic shock. Axial CT image acquired during portal venous phase shows a large saccular aneurysm of the hepatic artery compressing the portal vein (arrowhead). Courtesy of Dragan Vasin, MD; Department of Diagnostic Imaging, Clinical Center of Serbia, Belgrade, Serbia. **b**, **c** Axial CT images acquired during arterial phase in a different patient with vasculitis shows a large fusiform aneurysm of the hepatic artery, causing intrahepatic bile duct dilation (arrowheads) and an additional aneurysm of the left hepatic artery

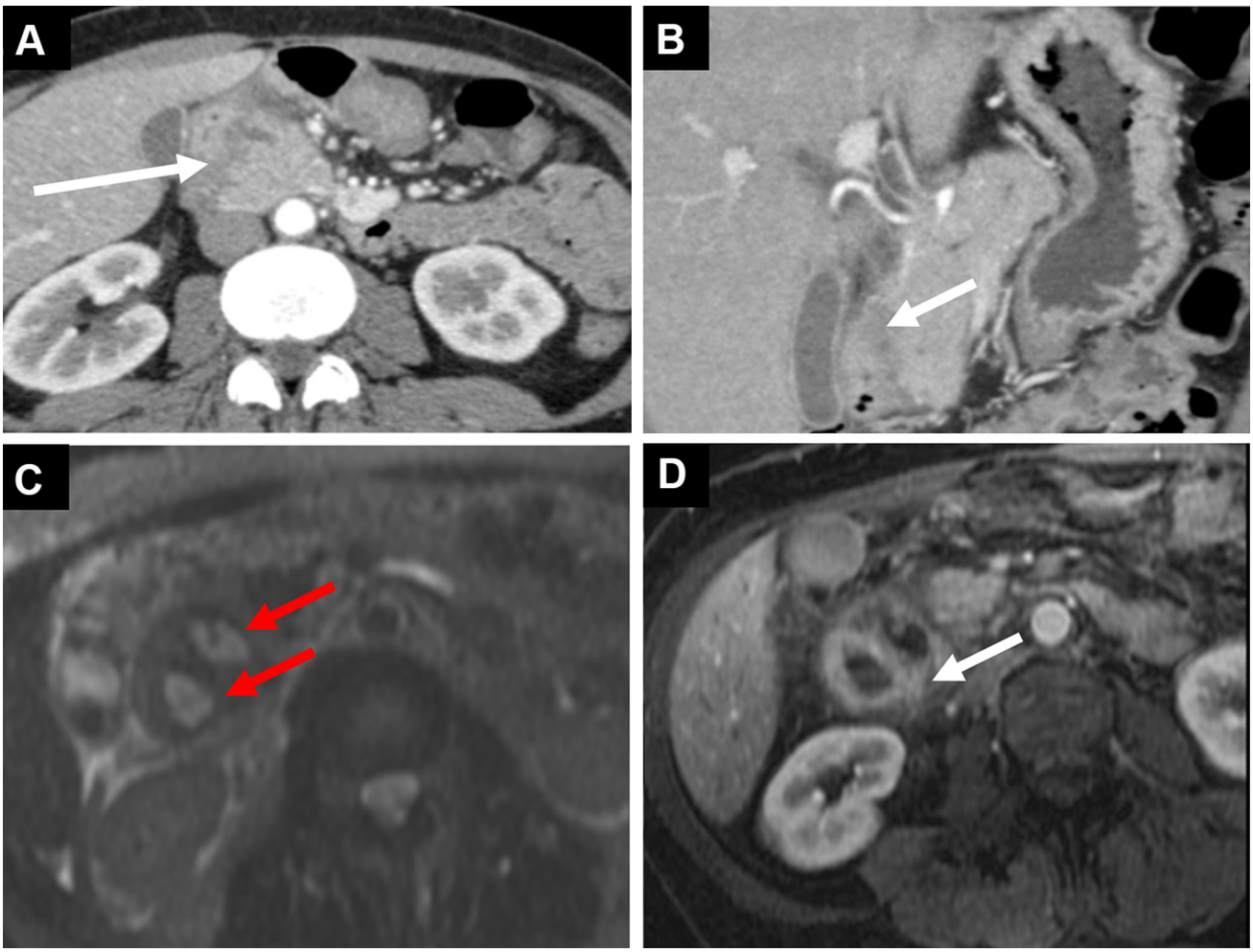

Fig. 24 Groove pancreatitis in a 37-year-old woman with abdominal pain. Contrast-enhanced axial (**a**) and MPR coronal reformatted (**b**) CT images obtained during late arterial phase, T2-weighted axial image (**c**) and contrast-enhanced T1-weighted axial image obtained during portal venous phase (**d**), show an inflammatory mass with multiple T2 hyperintense cysts in the duodenal wall (red arrows), fat stranding and inflammatory change in the pancreatic groove (white arrows), consistent with groove pancreatitis

MRCP shows the mildly hypointense "sheetlike" crescentic soft tissue on T1 weighted images, with variable signal intensity on T2-weighted images, depending on the acuity of the process. Duodenal wall thickening and multiple T2 hyperintense cysts in the duodenal wall and pancreaticoduodenal groove can be seen (Fig. 24). Abnormalities of the distal CBD and downstream pancreatic duct, both of which tend to be narrowed near the ampulla can be appreciated. A dilated gallbladder can be appreciated due to narrowing of the CBD (Fig. 24) [76, 77].

Acute pancreatitis

Acute peripancreatic fluid collections and acute necrotic collections may extend from the pancreas to involve the HDL (Fig. 25) [79]. Pseudocysts involving the HDL have also been reported, either invading the portal vein (termed pancreaticoportal vein fistula), or running into the omentum with intrahepatic pseudocyst formation (Fig. 26) [80]. Both these conditions can be diagnosed with MRCP, which shows either a T2-weighted hyperintense fluid collection within the portal vein or a fluid-filled HDL [81]. Sometimes progressive narrowing of the CBD due to extrinsic compression can occur (Fig. 27). On contrast-enhanced MDCT a thickened edematous hypodense HDL can be seen [80, 82].

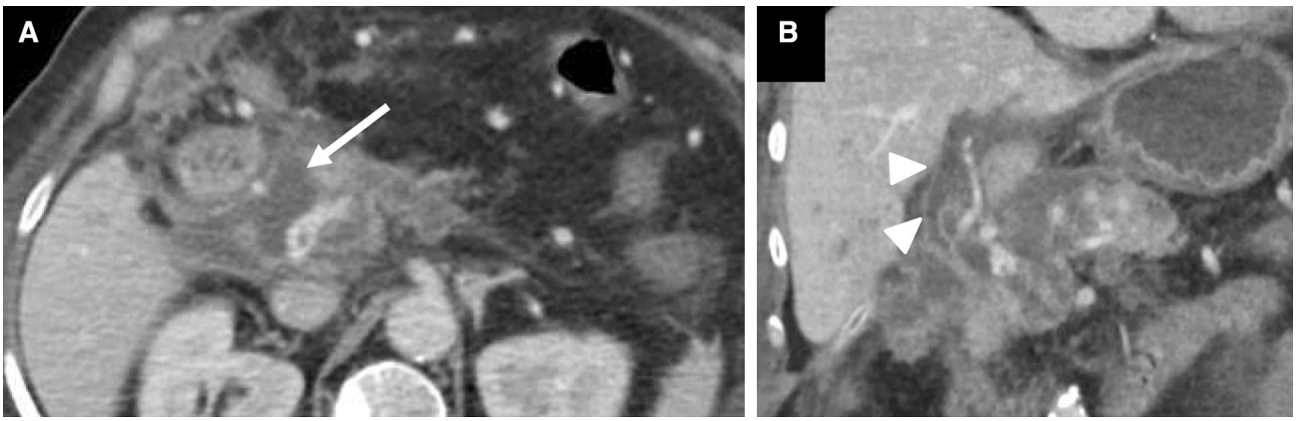

Fig. 25 Axial (**a**) and coronal (**b**) reconstructed CT image acquired during portal venous phase shows a hypodense collection (arrows) extending from the pancreatic head along the hepatoduodenal ligament (arrowheads) in a patient with necrotizing pancreatitis. Courtesy of Dragan Vasin, MD; Department of Diagnostic Imaging, Clinical Center of Serbia, Belgrade, Serbia

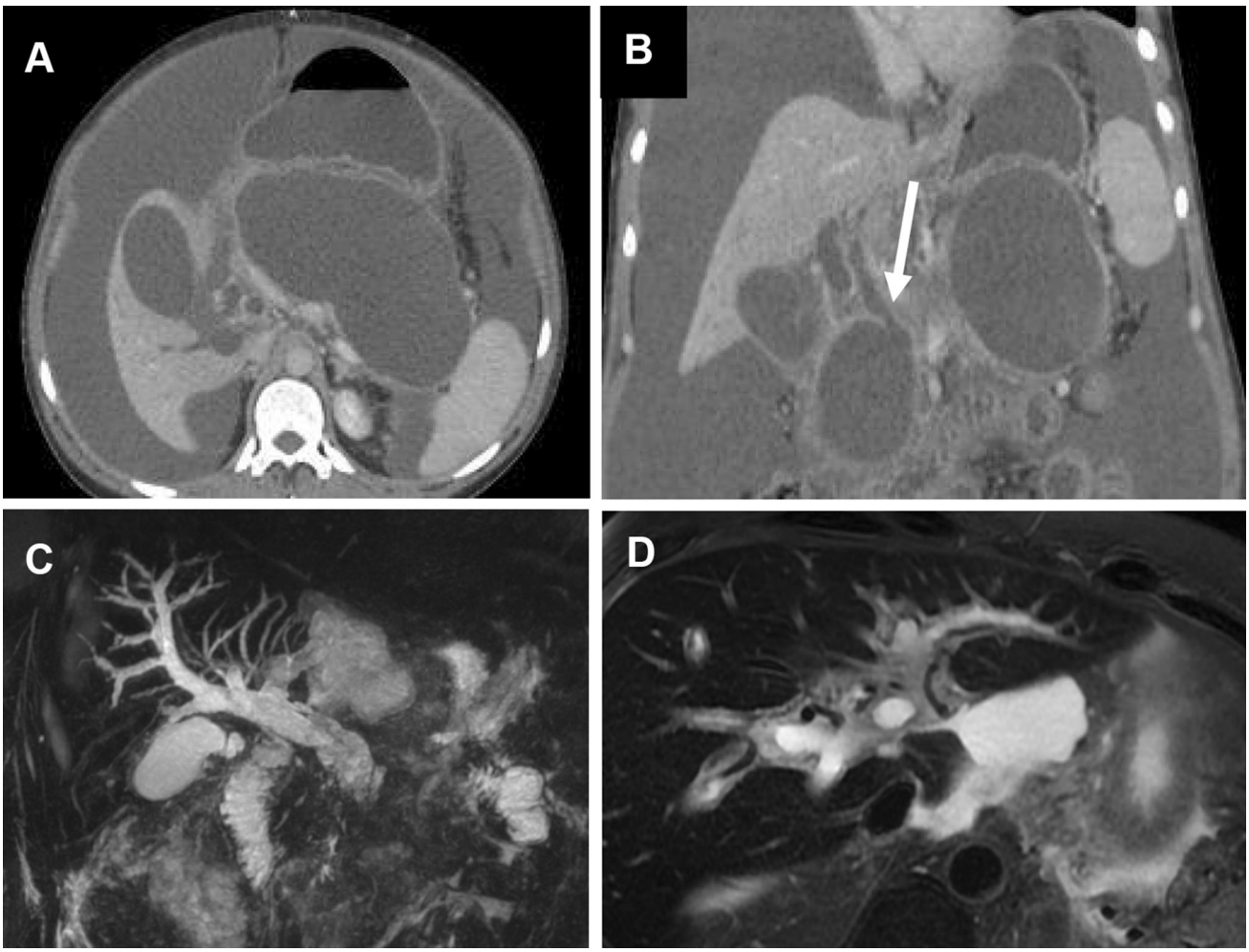

Fig. 26 Pancreatic pseudocyst-portal vein fistula. **a** Axial CT image acquired during portal venous phase shows a large pseudocyst along the lesser omentum and a diffusely hypodense portal vein, and a dilated common bile duct, **b** Coronal reconstructed CT image shows the communication between the portal vein and the pseudocyst (arrow). Courtesy of Dragan Vasin, MD; Department of Diagnostic Imaging, Clinical Center of Serbia, Belgrade, Serbia. **c** 3D MRCP in a different patient with acute pancreatitis shows a highly T-2 hyperintense portal vein. **d** T2 weighted fat suppressed axial image shows a fluid collection anterior to the portal vein and fluid extending into the portal vein and its branches

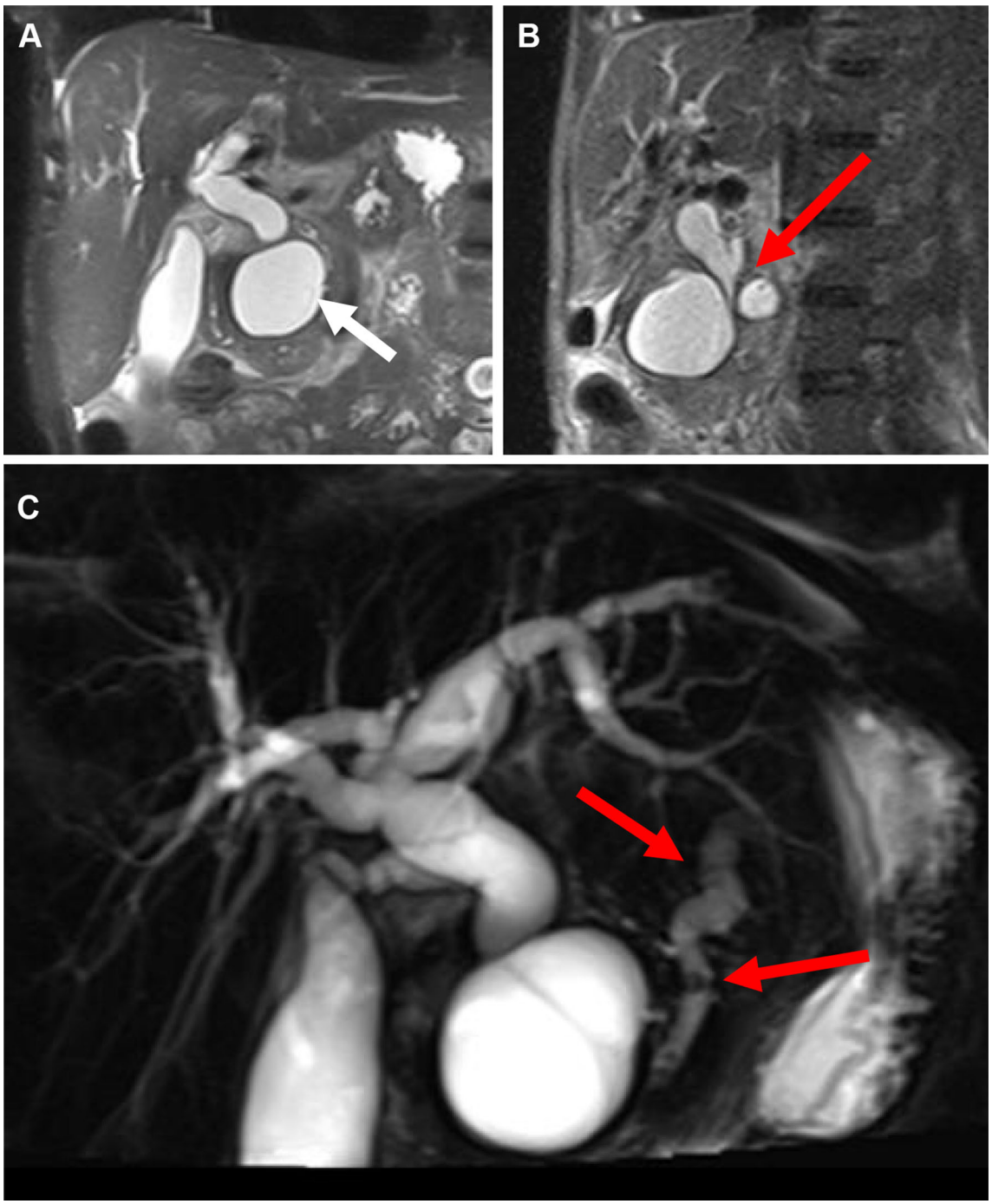

Fig. 27 Narrowing of the CBD due to extrinsic compression in a 72-years-old man with history of chronic pancreatitis and epigastric pain. **a** Coronal T2-weighted image show significant intrahepatic bile duct dilatation and large pseudocyst within the pancreatic head (white arrow) (**a**) extending along the HDL. **b** Sagittal T2-weighted image demonstrate progressive narrowing of the CBD due to extrinsic compression (red arrow). **c** Single-shot coronal MRCP image reveal ectasia and irregularity of the main pancreatic duct (red arrows) (**c**)

Conclusions

The HDL is an anatomically complex region in which a wide spectrum of non-neoplastic conditions can occur, including inflammatory and infectious diseases. Familiarity with MDCT and MRCP anatomy and awareness of the various processes that can occur within this region are mandatory to reach an accurate diagnosis.

Compliance with ethical standards

Conflict of interest Francesco Alessandrino declares that he has no conflict of interest. Aleksandar M. Ivanovic declares that he has no conflict of interest. Author Daniel Souza declares that he has no conflict of interest. Amin S. Chaoui declares that he has no conflict of interest. Jelena Djokic-Kovac declares that she has no conflict of interest. Koenraad J. Mortele declares that he has no conflict of interest.

Ethical approval This article does not contain any studies with human participants or animals performed by any of the authors.

Informed consent Statement of informed consent is not applicable since the manuscript does not contain any patient data.

References

1. Yoo E, Kim JH, Kim MJ, et al. (2007) Greater and lesser omenta: normal anatomy and pathologic processes. Radiographics 27(3):707–720
2. Lee SL, Lee HH, Ko YH, et al. (2014) Relevance of hepatoduodenal ligament lymph nodes in resectional surgery for gastric cancer. Br J Surg 101(5):518–522
3. DeMeo JH, Fulcher AS, Austin RF Jr (1995) Anatomic CT demonstration of the peritoneal spaces, ligaments, and mesenteries: normal and pathologic processes. Radiographics 15(4):755–770
4. Arenas AP, Sanchez LV, Albillos JM, Borruel SN, Roldán JR, Lozano FO (1994) Direct dissemination of pathologic abdominal processes through perihepatic ligaments: identification with CT. Radiographics 14(3):515–528
5. Tirumani SH, Shanbhogue AK, Vikram R, Prasad SR, Menias CO (2014) Imaging of the porta hepatis: spectrum of disease. Radiographics 34:73–92
6. Tirkes T, Sandrasegaran K, Patel AA, et al (2012) Peritoneal and retroperitoneal anatomy and its relevance for cross-sectional imaging. Radiographics 32:437–451
7. Weinstein JB, Heiken JP, Lee JK, et al. (1986) High resolution CT of the porta hepatis and hepatoduodenal ligament. Radiographics 6:55–74
8. Gadzijev EM (2002) Surgical anatomy of hepatoduodenal ligament and hepatic hilus. J Hepatobiliary Pancreat Surg 9(5):531–533
9. Röthlin M, Largiadèr F (1994) The anatomy of the hepatoduodenal ligament in laparoscopic sonography. Surg Endosc 8(3):173–180
10. Flint ER (1923) Abnormalities of the right hepatic, cystic and gastroduodenal arteries, and of bile-ducts. Br J Surg 10:509–519
11. Weiglein AH (1996) Variations and topography of the arteries in the lesser omentum in humans. Clin Anat 9(3):143–150
12. Mortelé KJ, Ros PR (2001) Anatomical variants of the biliary tree: MR cholangiographic findings and clinical applications. AJR 177:389–394
13. Ramesh Babu CS, Sharma M (2014) Biliary tract anatomy and its relationship with venous drainage. JClin Exp Hepatol 4:S18–S26
14. Dhiman RK, Behera A, Chawla YK, Dilawari JB, Suri S (2007) Portal hypertensive biliopathy. Gut 56(7):1001–1008
15. Okada Y, Yao YK, Yunoki M, Sugita T (1996) Lymph nodes in the hepatoduodenal ligament: US appearances with CT and MR correlation. Clin Radiol 51(3):160–166
16. Gallego C, Velasco M, Marcuello P, Tejedor D, De Campo L, Friera A (2002) Congenital and acquired anomalies of the portal venous system. Radiographics 22(1):141–159
17. McNaughton DA, Abu-Yousef MM (2011) Doppler US of the liver made simple. Radiographics. 31(1):161–188
18. Einstein DM, Singer AA, Chilcote WA, Desai RK (1997) Abdominal lymphadenopathy: spectrum of CT findings. Radiographics 11(3):457–472
19. Ito K, Higuchi M, Kada T, et al. (1997) CT of acquired abnormalities of the portal venous system. Radiographics 17(4):897–917
20. Lassanfro F, Romano S, Ragozzino A, et al. (2005) Clinical observations: role of helical CT in diagnosis of gallstone ileus and related conditions. AJR 185(5):1159–1165
21. O'Connor OJ, O'Neill S, Maher MM (2011) Imaging of biliary tract disease. AJR 197(4):W551–558
22. Mortelé KJ, Rocha TC, Streeter JL, Taylor AJ (2006) Multimodality imaging of pancreatic and biliary congenital anomalies. Radiographics 26(3):715–731
23. Katabathina VS, Dasyam AK, Dasyam N, Hosseinzadeh K (2014) Adult bile duct strictures: role of MR imaging and MR cholangiopancreatography in characterization. Radiographics 34(3):565–586
24. Metreweli C, Ward SC (1995) Ultrasound demonstration of lymph nodes in the hepatoduodenal ligament ('daisy chain nodes') in normal subjects. Clinical Radiology 50:99–101
25. Lyttkens K, Forsberg L, Henderström E (1990) Ultrasound examination of lymph nodes in the hepato-duodenal ligament. Br J Radiol 63(745):26–30
26. Dodd GD 3rd, Baron RL, Oliver JH 3rd, Federle MP, Baumgartel PB (1997) Enlarged abdominal lymph nodes in end-stage cirrhosis: CT-histopathologic correlation in 507 patients. Radiology 203(1):127–130
27. Lucey BC, Stuhlfaut JW, Soto JA (2005) Mesenteric lymph nodes: detection and significance on MDCT. AJR 184(1):41–44
28. Lucey BC, Stuhlfaut JW, Soto JA (2005) Mesenteric lymph nodes seen at imaging: causes and significance. Radiographics 25(2):351–365
29. Muller P, Renou C, Harafa A, et al. (2003) Lymph node enlargement within the hepatoduodenal ligament in patients with chronic hepatitis C reflects the immunological cellular response of the host. J Hepatol 39(5):807–813
30. Lee WK, Van Tonder F, Tartaglia CJ, et al. (2012) CT appearances of abdominal tuberculosis. Clin Radiol 67(6):596–604
31. Li Y, Yang ZG, Guo YK, et al. (2007) Distribution and characteristics of hematogenous disseminated tuberculosis within the abdomen on contrast-enhanced CT. Abdom Imaging 32(4):484–488
32. Yang ZG, Min PQ, Sone S, et al. (1999) Tuberculosis versus lymphomas in the abdominal lymph nodes: evaluation with contrast-enhanced CT. AJR 172(3):619–623
33. Pereira JM, Madureira AJ, Vieira A, Ramos I (2005) Abdominal tuberculosis: imaging features. Eur J Radiol 55(2):173–180
34. De Backer AI, Mortelé KJ, Deeren D, Vanschoubroeck IJ, De Keulenaer BL (2005) Abdominal tuberculous lymphadenopathy: MRI features. Eur Radiol 15(10):2104–2109
35. Todani T, Watanabe Y, Narusue M, Tabuchi K, Okajima K (1977) Congenital bile duct cysts: classification, operative procedures, and review of thirty-seven cases including cancer arising from choledochal cyst. Am J Surg 134(2):263–269
36. Wiseman K, Buczkowski AK, Chung SW, et al. (2005) Epidemiology, presentation, diagnosis, and outcomes of choledochal cysts in adults in an urban environment. Am J Surg 189(5):527–531
37. Law R, Topazian M (2014) Diagnosis and treatment of choledochoceles. Clin Gastroenterol Hepatol 12(2):196–203
38. Csendes A, Díaz JC, Burdiles P, Maluenda F, Nava O (1989) Mirizzi syndrome and cholecystobiliary fistula: a unifying classification. Br J Surg 76(11):1139–1143

39. Yun EJ, Choi CS, Yoon DY, et al. (2009) Combination of magnetic resonance cholangiopancreatography and computed tomography for preoperative diagnosis of the Mirizzi syndrome. J Comput Assist Tomogr 33(4):636–640
40. Chick JF, Chauhan NR, Mandell JC, et al. (2013) Traffic jam in the duodenum: imaging and pathogenesis of Bouveret syndrome. J Emerg Med 45(4):e135–137
41. Cappell MS, Davis M (2006) Characterization of Bouveret's syndrome: a comprehensive review of 128 cases. Am J Gastroenterol 101:2139–2146
42. Walser EM, Runyan BR, Heckman MG, et al. (2010) Extrahepatic portal biliopathy: proposed etiology on the basis of anatomic and clinical features. Radiology 258(1):146–153
43. Aguirre DA, Farhadi FA, Rattansingh A, Jhaveri KS (2012) Portal biliopathy: imaging manifestations on multidetector computed tomography and magnetic resonance imaging. Clin Imaging 36(2):126–134
44. Besa C, Cruz JP, Huete A, Cruz F (2012) Portal biliopathy: a multitechnique imaging approach. Abdom Imaging 37(1):83–90
45. Condat B, Vilgrain V, Asselah T, et al. (2003) Portal cavernoma-associated cholangiopathy: a clinical and MR cholangiography coupled with MR portography imaging study. Hepatology 37(6):1302–1308
46. Shin SM, Kim S, Lee JW, et al. (2007) Biliary abnormalities associated with portal biliopathy: evaluation on MR cholangiography. AJR 188(4):W341–W347
47. Chong VH, Chong CF (2010) Biliary complications secondary to post-cholecystectomy clip migration: a review of 69 cases. J Gastrointest Surg 14(4):688–696
48. Girometti R, Brondani G, Cereser L, et al. (2010) Post-cholecystectomy syndrome: spectrum of biliary findings at magnetic resonance cholangiopancreatography. Br J Radiol 83(988):351–361
49. Hoeffel C, Azizi L, Lewin M, et al. (2006) Normal and pathologic features of the postoperative biliary tract at 3D MR cholangiopancreatography and MR imaging. Radiographics 26(6):1603–1620
50. Turner MA, Fulcher AS (2001) The Cystic Duct: normal Anatomy and Disease Processes. Radiographics 21(1):3–22
51. Laghi A, Pavone P, Catalano C, et al. (1999) MR cholangiography of late biliary complications after liver transplantation. AJR 172(6):1541–1546
52. Deltenre P, Valla DC (2006) Ischemic cholangiopathy. J Hepatol 44(4):806–817
53. Camacho JC, Coursey-Moreno C, Telleria JC, et al. (2015) Nonvascular post-liver transplantation complications: from US screening to cross-sectional and interventional imaging. Radiographics 35(1):87–104
54. Ratcliffe GE, Kirkpatrick ID, Anik Sahni V, et al. (2014) Detection and localization of bile duct leaks after cholecystectomy using Gd-EOB-DTPA-enhanced MR cholangiography: retrospective study of 16 patients. J Comput Assist Tomogr 38(4):518–525
55. Cieszanowski A, Stadnik A, Lezak A, et al. (2013) Detection of active bile leak with Gd-EOB-DTPA enhanced MR cholangiography: comparison of 20-25 min delayed and 60–180 min delayed images. Eur J Radiol 82(12):2176–2182
56. Catalano OA, Sahani DV, Forcione DG, et al. (2009) Biliary infections: spectrum of imaging findings and management. Radiographics 29(7):2059–2080
57. Patel NB, Oto A, Sn Thomas (2013) Multidetector CT of emergent biliary pathologic conditions. Radiographics 33(7):1867–1888
58. Khuroo MS, Zargar SA, Mahajan R (1990) Hepatobiliary and pancreatic ascariasis in India. Lancet 335(8704):1503–1506
59. Lim JH, Kim SY, Park CM (2007) Parasitic diseases of the biliary tract. AJR 188(6):1596–1603
60. Das CJ, Kumar J, Debnath J, Chaudhry A (2007) Imaging of ascariasis. Australas Radiol 51(6):500–506
61. Khuroo MS, Zargar SA, Mahajan R, Bhat RL, Javid G (1987) Sonographic appearance in biliary ascariasis. Gastroenterology 93:267–272
62. Czermak BV, Akhan O, Hiemetzberger R, et al. (2008) Echinococcosis of the liver. Abdom Imaging 33(2):133–143
63. Ortega CD, Ogawa NY, Rocha MS, et al. (2010) Helminthic diseases in the abdomen: an epidemiologic and radiologic overview. Radiographics 30(1):253–267
64. Chaudhary P (2014) Hepatobiliary tuberculosis. Ann Gastroenterol 27(3):207–211
65. Ramanampamonjy RM, Ramarozatovo LS, Bonnet F, et al. (2005) Portal vein thrombosis in HIV-infected patients: report of four cases. Rev Med Interne 26(7):545–548
66. Tonolini M, Bianco R (2013) HIV-related/AIDS cholangiopathy: pictorial review with emphasis on MRCP findings and differential diagnosis. Clin Imaging 37(2):219–226
67. Chawla Y, Duseja A, Dhiman RK (2009) Review article: the modern management of portal vein thrombosis. Aliment Pharmacol Ther 30(9):881–894
68. Hidajat N, Stobbe H, Griesshaber V, Felix R, Schroder RJ (2005) Imaging and radiological interventions of portal vein thrombosis. Acta Radiol 46(4):336–343
69. Lupescu I, Masala N, Capsa R, Câmpeanu N, Georgescu SA (2006) CT and MRI of acquired portal venous system anomalies. Journal of Gastrointestinal and Liver Diseases 15(4):393–398
70. Wozney P, Zajko AB, Bron KM, Point S, Starzl TE (1986) Vascular complications after liver transplantation: a 5-year experience. AJR 147(4):657–663
71. Dalal PS, Raman SP, Horton KM, Fishman EK (2013) Portal vein aneurysms: imaging manifestations and clinical significance. Emerg Radiol 20(5):453–457
72. Koc Z, Oguzkurt L, Ulusan S (2007) Portal venous system aneurysms: imaging, clinical findings, and a possible new etiologic factor. AJR 189(5):1023–1030
73. Abboud B, El Hachem J, Yazbeck T, Doumit C (2009) Hepatic portal venous gas: physiopathology, etiology, prognosis and treatment. World J Gastroenterol 15(29):3585–3590
74. Lu M, Weiss C, Fishman EK, Johnson PT, Verde F (2015) Review of visceral aneurysms and pseudoaneurysms. J Comput Assist Tomogr 39(1):1–6
75. Stolte M, Weiss W, Volkholz H, Rösch W (1982) A special form of segmental pancreatitis: "groove pancreatitis". Hepatogastroenterology 29(5):198–208
76. Hungerford JP, Neill Magarik MA, Hardie AD (2015) The breadth of imaging findings of groove pancreatitis. Clin Imaging . https://doi.org/10.1016/j.clinimag.2015.01.018
77. Raman SP, Salaria SN, Hruban RH, Fishman EK (2013) Groove pancreatitis: spectrum of imaging findings and radiology-pathology correlation. AJR 201(1):W29–39
78. Itoh S, Yamakawa K, Shimamoto K, Endo T, Ishigaki T (1994) CT findings in groove pancreatitis: correlation with histopathological findings. J Comput Assist Tomogr 18(6):911–915
79. Murphy KP, O'Connor OJ, Maher MM (2014) Updated imaging nomenclature for acute pancreatitis. AJR 203(5):W464–469
80. Shibasaki M, Bandai Y, Ukai T (2002) Pancreatic pseudocyst extending into the liver via the hepatoduodenal ligament: a case report. Hepatogastroenterology 49(48):1719–1721
81. Alessandrino F, Strickland C, Mojtahed A, Eberhardt SC, Mortele KJ (2017) Clinical and cross-sectional imaging features of spontaneous pancreatic pseudocyst-portal vein fistula. Clin Imaging 44:22–26
82. Dayal M, Sharma R, Madhusudhan KS, Garg PK (2014) MRI diagnosis of rupture of pancreatic pseudocyst into portal vein: case report and review of literature. Ann Gastroenterol 27(2):173–176